Numerical approximations
of a lattice Boltzmann scheme
with a family of partial differential equations

Bruce M. Boghosian[ab], François Dubois[cd] and Pierre Lallemand[e]

[a] *Department of Mathematics, Tufts University, Medford, MA, 02155, USA.*
[b] *present address: American University of Armenia,*
40 Baghramyan Avenue, Yerevan 0019, Armenia.
[c] *Laboratoire de Mathématiques d'Orsay, Faculté des Sciences d'Orsay,*
Université Paris-Saclay, France.
[d] *Conservatoire National des Arts et Métiers, LMSSC laboratory, Paris, France.*
[e] *Beijing Computational Science Research Center, Haidian District, Beijing 100094, China.*

27 March 2024 [*]

Abstract

Is it possible to consider a lattice Boltzmann scheme as an approximation of a partial differential equation? For a nonhomogeneous advection problem in one spatial dimension, we propose equivalent partial differential equations at various orders. We compare the lattice Boltzmann results and a spectral approximation of the differential equations. No simple correlation is obtained for a stationary problem. For an unsteady situation, we show that the initialization scheme of the microscopic moments plays a crucial role.

---

[*] This contribution has been presented at the 19th International Conference for Mesoscopic Methods in Engineering and Science, Mount Qing-Cheng (Chengdu, Sichuan, China) the 25 July 2023 and at Institut Henri Poincaré the 04 October 2023.

BRUCE M. BOGHOSIAN, FRANÇOIS DUBOIS AND PIERRE LALLEMAND

1) Introduction

The classical framework for the art of scientific computing starts from partial differential equations. After discretization with some numerical method (finite differences, finite elements, *etc.*), numerical software is developed. Then an approximate solution of the original partial differential equation is computed. A large number of high-quality books exist on this subject. We refer to the works of Oden and Reddy [25], Ferziger and Perić [14], Lucquin and Pironneau [23], among others.

With cellular automata and lattice Boltzmann schemes, this paradigm is reversed. The computing algorithm is the starting point of the study. Then an asymptotic analysis is conducted to derive the underlying continuous equations. The reader can consult, *e.g.*, the books of Rothman and Zaleski [28], Succi [30], Guo and Shu [16], or Krüger *et al.* [21].

In order to define a physical model from the algorithm, the classical approach is the Chapman-Enskog method [5]. It has been revisited in [6, 27] to take into consideration the discrete aspects of space and time with cellular automata and lattice Boltzmann schemes. We have suggested using Taylor expansions to derive equivalent partial differential equations [7, 8]. We have also established that this Taylor expansion method is equivalent to the Chapman-Enskog approach [10].

When an asymptotic partial differential equation is known, it is possible to fit some parameters of the scheme to obtain super convergence. This was done by d'Humières and Ginzburg [20], and by our team in [1, 11, 12, 26]. We apply this type of idea in the present contribution.

In this work, we adopt the paradigm of multirelaxation lattice Boltzmann schemes [18], and we have a methodology [9, 10] to develop an asymptotic analysis. Thus an important question is the comparison between the simulation with a lattice Boltzmann scheme and reference solutions of the equivalent partial differential equations. In this contribution, the work is done with an elementary D1Q3 one-dimensional lattice Boltzmann scheme and a simple spectral approach to solve numerically with great precision the family of equivalent partial differential equations at various orders.

The outline for this work is as follows. In Section 2, we study the reference model: the advection equation in one spatial dimension with a given cosine velocity field. The method of characteristics yields an analytic solution. In Section 3, we present our variant of the D1Q3 lattice Boltzmann scheme, introduced initially by Broadwell [4] in the context of simple discrete-velocity gases. In the lattice Boltzmann framework, dynamics is captured with particles and the relaxation process occurs in the space of moments [18]. They are divided into two families: the conserved moments and the microscopic variables in the denomination proposed by Gatignol [15]. Then we present the "ABCD" asymptotic analysis [9, 10]. From the precise algebraic expression of a multirelaxation lattice Boltzmann scheme [18, 19], we derive from a formal exponential expression a set of equivalent partial differential equations up to fourth order accuracy. Here we adapt the underlying algebra first to the case of a non-homogeneous linear partial differential equation, and second to the D1Q3 lattice Boltzmann model. In Section 5, the Fourier series method is adapted to treat in a precise way the case

of an cosine advective field. A long-time asymptotic analysis is presented in Section 6. We present various numerical experiments with several values of the velocity field and refining meshes. Then the unsteady evolution is presented in Section 7. A first result is relative to a constant velocity and an initial sine wave. Then we take into account a cosine advection velocity with a sinus or a constant initial condition. An interesting phenomenon of lack of convergence is encountered. This motivates the next Section relative to the initialization of microscopic moments. In the last Section, we present our numerical experiments with a detailed asymptotic analysis. Various parameters are considered: the type of problem, with constant or cosine advective velocity, the approximation order of the partial differential equation, the number of mesh points and the initialization process.

This work is the result of conversations in Medford (MA, USA) in summer 2018, then in Paris in spring 2019. Independent numerical experiments were done during the covid in spring 2020, and complementary work in Beijing in summer 2023.

2) Advection with harmonic velocity in one space dimension

We introduce a reference length $L > 0$ and a reference scale velocity $\lambda > 0$. For a given scalar $U \in \mathbb{R}$ and for $0 \leq x \leq L$, we consider the regular periodic velocity field

$$(1) \qquad\qquad u(x) = \lambda\, U\, \cos(k\, x)\,, \quad k = \frac{2\pi}{L}.$$

The linear inhomogeneous advection equation is the first-order partial differential equation

$$(2) \qquad\qquad \frac{\partial \rho}{\partial t} + \lambda \frac{\partial}{\partial x}\big[U\, \cos(k\, x)\, \rho\big] = 0.$$

We introduce a periodic function $[0, L] \ni x \longmapsto \rho_0(x) \in \mathbb{R}$ as an initial condition

$$(3) \qquad\qquad \rho(x,\, 0) = \rho_0(x).$$

Moreover, we suppose periodic boundary conditions throughout this study.

Proposition 1. Method of characteristics
The differential equation associated with the method of characteristics for the partial differential equation (2) is written

$$(4) \qquad\qquad \frac{\mathrm{d}X}{\mathrm{d}t} = \lambda\, u(X(t)) \equiv \lambda\, U\, \cos\big(k\, X(t)\big).$$

With the initial condition $X(0) = x_0$ with $0 \leq x_0 \leq L$, the solution is:

$$(5) \qquad\qquad \operatorname{cotg}\frac{\pi\, X}{L} = \frac{\operatorname{th}\frac{\pi\, t}{T} + \operatorname{cotg}\frac{\pi\, x_0}{L}}{1 + \operatorname{th}\frac{\pi\, t}{T}\, \operatorname{cotg}\frac{\pi\, x_0}{L}}$$

with $\lambda\, U \equiv \frac{L}{T}$, $\operatorname{th}\varphi \equiv \dfrac{\exp\varphi - \exp(-\varphi)}{\exp\varphi + \exp(-\varphi)}$ and $\operatorname{cotg}\varphi \equiv \dfrac{1}{\tan\varphi}$.

Proof of Proposition 1.
If $t = 0$, then $\operatorname{cotg}\frac{\pi\, X}{L} = \operatorname{cotg}\frac{\pi\, x_0}{L}$ and $\pi\, \frac{X - x_0}{L}$ is a multiple of π. Then the position $X = x_0$ is well defined in the interval $[0,\, L]$. Moreover, we have the following calculus:

$$-\frac{1}{\sin^2\frac{\pi\, X}{L}}\, \frac{\pi}{L}\, \frac{\mathrm{d}X}{\mathrm{d}t} = \frac{\pi}{T}\, \frac{(1 - \operatorname{th}^2\frac{\pi\, t}{T})\,(1 - \operatorname{cotg}^2\frac{\pi\, x_0}{L})}{(1 + \operatorname{th}\frac{\pi\, t}{T}\, \operatorname{cotg}\frac{\pi\, x_0}{L})^2} = -\frac{\pi}{T}\, \frac{1}{\sin^2\frac{\pi\, X}{L}}\, \cos\frac{2\, \pi\, X}{L}$$

Then $\frac{\mathrm{d}X}{\mathrm{d}t} = \frac{L}{T}\, \cos\frac{2\, \pi\, X}{L}$ and the differential equation (4) is satisfied. $\qquad\square$

Proposition 2. Algebraic solution of the inhomogeneous advection equation
Given $x \in [0, L]$ and $t > 0$, the solution $\rho(x, t)$ of the equation (2) satisfying the initial condition (3) is given by the relation

$$\rho(x, t) \cos\left(\frac{2\pi x}{L}\right) = \rho_0(x_0) \cos\left(\frac{2\pi x_0}{L}\right)$$

where x_0 satisfies

(6)
$$\cotg\frac{\pi x_0}{L} = \frac{\cotg\frac{\pi x}{L} - \th\frac{\pi t}{T}}{1 - \th\frac{\pi t}{T}\cotg\frac{\pi x_0}{L}}.$$

Proof of Proposition 2.
We search the foot x_0 of the characteristic $t \longmapsto X(t)$ (4) such that $X(0) = x_0$ and $X(t) = x$. First, we deduce from the partial differential equation (2) that the product $\rho(x, t) \cos\left(\frac{2\pi x}{L}\right)$ remains constant. Second, from the relation (5), we deduce the relation (6) for defining x_0. □
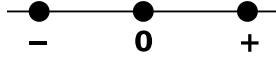

Figure 1: D1Q3 lattice Boltzmann scheme

3) D1Q3 lattice Boltzmann scheme

The scale velocity $\lambda > 0$ is now equal to the ratio between the space step Δx and the time step Δt:

$$\lambda = \frac{\Delta x}{\Delta t}.$$

From the particle distribution $f \equiv (f_+, f_0, f_-)^{\mathrm{t}}$ presented in Figure 1, we construct a single conserved moment W denoted "density" in the following: $\rho = f_+ + f_0 + f_-$. We have also two non-conserved microscopic moments $Y = (J, e)^{\mathrm{t}}$ with the "momentum" $J = \lambda f_+ - \lambda f_-$ and the "energy" $e = \lambda^2 (f_+ - 2 f_0 + f_-)$. Then the family of moments $m \equiv (W, Y)$ is linked to the particles f with the d'Humières [18] matrix M: $m \equiv M f$, with

$$M = \begin{pmatrix} 1 & 1 & 1 \\ \lambda & 0 & -\lambda \\ \lambda^2 & -2\lambda^2 & \lambda^2 \end{pmatrix}.$$

For an inhomogeneous linear equilibrium $Y^{\mathrm{eq}} = \Phi(W) = E(x) W$, the equilibrium matrix $E(x)$ is a function of space. In the case of an advective field $u(x)$ proposed in the relation (1), we have

$$E(x) = \begin{pmatrix} \lambda U \cos(k x) \\ \lambda^2 \alpha \end{pmatrix}$$

with a coefficient $\alpha = -1$ in our numerical experiments.

The relaxation $Y \longmapsto Y^*$ of the nonconserved moments Y is classical:

$$\begin{cases} J^* = J + s\,(J^{\mathrm{eq}} - J) = (1 - s)\,J + s\,\lambda U \cos(k x)\,\rho \\ e^* = e + s'\,(e^{\mathrm{eq}} - e) = (1 - s')\,e + s'\,\lambda^2 \alpha\,\rho \end{cases}$$

and we have chosen $s = 1.5$, $s' = 1.2$ in our reference numerical experiments. Observe that the parameters U, α, s and s' are without dimension. We set finally $m^* = (\rho, \, J^*, \, e^*)^{\mathrm{t}}$. The collision step is defined according to $f^* = M^{-1} m^*$, and the exact propagation of particles along the characteristic directions $\lambda, \, 0, \, -\lambda$ of the D1Q3 scheme:

$$\begin{cases} f_+(x, \, t + \Delta t) = f_+^*(x - \Delta x, \, t) \\ f_0(x, \, t + \Delta t) \, = f_0^*(x, \, t) \\ f_-(x, \, t + \Delta t) = f_-^*(x + \Delta x, \, t) \end{cases}$$

is well known (see *e.g.* [18]). The solution of this lattice Boltzmann scheme can be approached by the first order equivalent partial differential equation

$$\frac{\partial \rho}{\partial t} + \lambda \, \frac{\partial}{\partial x} \big[U \, \cos(k \, x) \, \rho \big] = \mathrm{O}(\Delta x).$$

Therefore, it is natural to compare the numerical solution of the D1Q3 lattice Boltzmann scheme with the exact solution of the nonhomogeneous advection equation (2). We have done this work in a first numerical experiment, and the results are displayed in Figure 2.
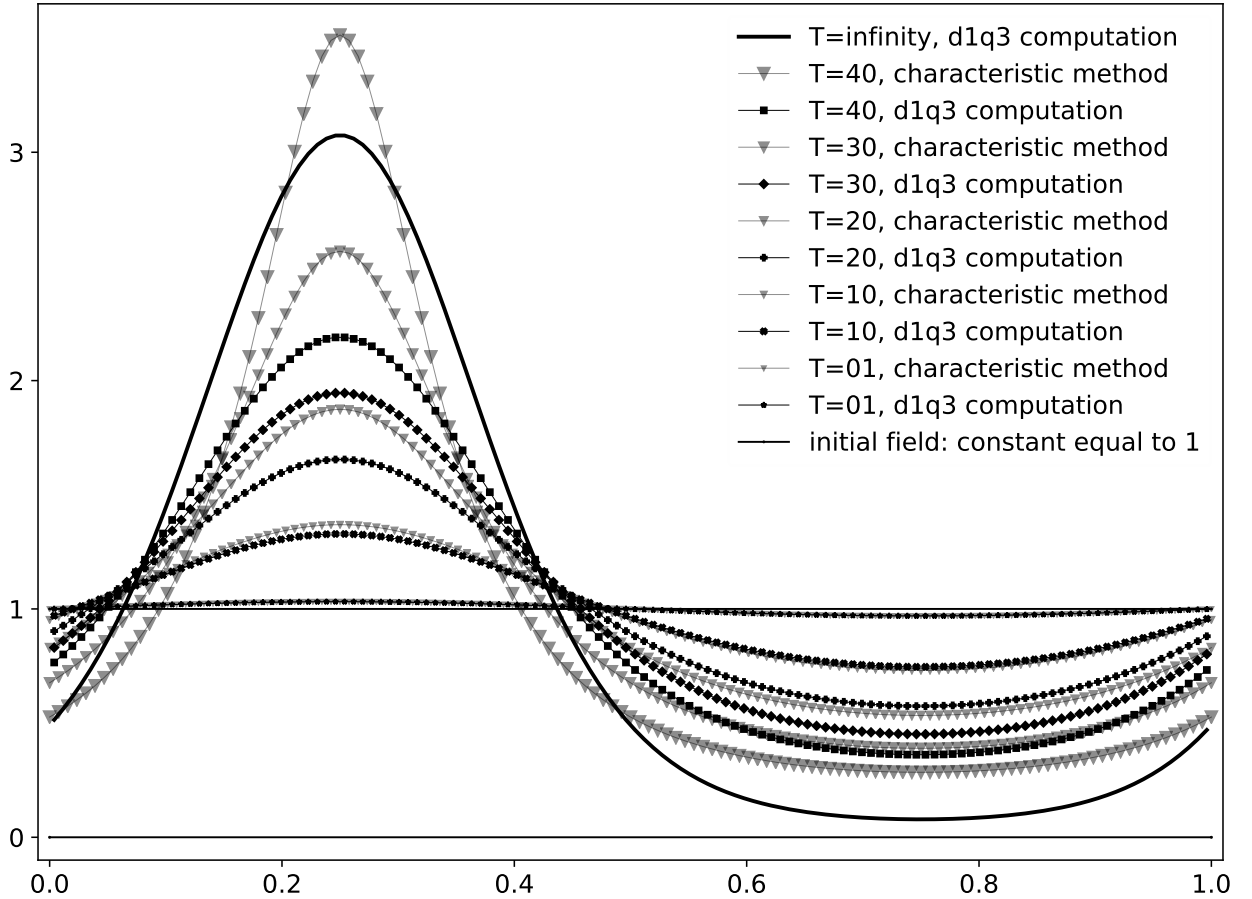

Figure 2: Evolution for an advective velocity (1) with $U = 0.005$ and $N = 128$ mesh points. We observe that with the cosine advection velocity, the numerical solution has no symmetry.

During the first time steps (see the results for $T = 01$ and $T = 10$), the two results agree with good precision. But we observe that the solution of the advection equation (2) is unsteady,

whereas the lattice Boltzmann scheme rapidly converges towards a stationary solution. Then the approximation of the D1Q3 scheme by the first-order partial differential equation is not sufficient. We adapt a complementary analysis in the next section.

4)   ABCD asymptotics in the isotropic linear case

In this section, we revisit the "Berlin algorithm" introduced in [2] for the linear analysis of lattice Boltzmann schemes. First recall that we have two steps for one time iteration:

(i) nonlinear relaxation

$$m \longmapsto m^* \equiv \begin{pmatrix} W^* \\ Y^* \end{pmatrix} , \ W^* = W , \ Y^* = Y + S\left(\Phi(W) - Y\right)$$

with a diagonal relaxation matrix S. For the D1Q3 scheme, we have $S = \mathrm{diag}(s, \, s')$.

(ii) linear advection

$$m^* \longmapsto f(t + \Delta t) : \ f^* = M^{-1} m^* , \ f_j(x, \, t + \Delta t) = f_j^*(x - v_j \, \Delta t, \, t).$$

The momentum-velocity operator matrix Λ is defined from the diagonal advection operator $\sum_\alpha v^\alpha \, \partial_\alpha$ according to [9]

$$\Lambda \equiv M \ \mathrm{diag}\Big(\sum_{1 \leq \alpha \leq d} v^\alpha \, \partial_\alpha \Big) M^{-1}$$

with d the spatial dimension. This is nothing more than the advection operator in the basis of moments. Following a remark proposed in [9], we have an exact exponential expression of the lattice Boltzmann scheme

$$m(x, t + \Delta t) = \exp(-\Delta t \, \Lambda) \, m^*(x, \, t).$$

We can expand this relation up to fourth order to obtain

$$m(x, t + \Delta t) = \left[\mathrm{I} - \Delta t \, \Lambda + \frac{\Delta t^2}{2} \Lambda^2 - \frac{\Delta t^3}{6} \Lambda^3 + \frac{\Delta t^4}{24} \Lambda^4 + \mathrm{O}(\Delta t^5) \right] m^*(x, \, t).$$

The equivalent partial differential equations of the scheme are found from the asymptotic expansion (see *e.g.* [10])

$$\partial_t = \partial_{t_1} + \Delta t \, \partial_{t_2} + \Delta t^2 \, \partial_{t_3} + \Delta t^3 \, \partial_{t_4} + \mathrm{O}(\Delta t^3).$$

Consider now the "ABCD" block decomposition (see [10]) of the momentum-velocity operator that is obtained for the D1Q3 lattice Boltzmann scheme:

$$\Lambda \equiv \begin{pmatrix} A & B \\ C & D \end{pmatrix} = \left(\begin{array}{c|cc} 0 & \partial_x & 0 \\ \hline \frac{2}{3}\lambda^2 \partial_x & 0 & \partial_x \\ 0 & \lambda^2 \partial_x & 0 \end{array} \right).$$

Asymptotic analysis is carried out to second order. It uses only a small set of algebraic expressions:

(7)
$$\begin{cases} \partial_{t_1} W + \Gamma_1 = 0 \\ \partial_{t_2} W + \Gamma_2 = 0 \\ \Gamma_1 = A \, W + B \, \Phi(W) \\ Y = \Phi(W) + \Delta t \, S^{-1} \, \Psi_1 + \mathrm{O}(\Delta t^2) \\ \Psi_1 = \mathrm{d}\Phi(W).\Gamma_1 - (C \, W + D \, \Phi(W)) \\ \Sigma \equiv S^{-1} - \frac{1}{2} \mathrm{I} \\ \Gamma_2 = B \, \Sigma \, \Psi_1. \end{cases}$$

The application to the Navier Stokes equations can be found in [13]. For the fourth-order analysis, these relations are enriched in the following way [9, 10]. We first extend the asymptotic expansion for the microscopic moments

(8) $$Y = \Phi(W) + S^{-1}\left(\Delta t\,\Psi_1(W) + \Delta t^2\,\Psi_2(W) + \Delta t^3\,\Psi_3(W)\right) + \mathrm{O}(\Delta t^4).$$

We observe that the operators Ψ_j are *a priori* nonlinear operators of order j. The partial differential equation for the conserved moments takes the form

$$\partial_{t_1}W + \Gamma_1 = 0\,,\ \ \partial_{t_2}W + \Gamma_2 = 0\,,\ \ \partial_{t_3}W + \Gamma_3 = 0\,,\ \ \partial_{t_4}W + \Gamma_4 = 0\,.$$

The differential operators at third order are obtained by nontrivial algebra [9, 10]:

(9) $$\begin{cases} \Psi_2(W) = \Sigma\,\mathrm{d}\Psi_1(W).\Gamma_1(W) + \mathrm{d}\Phi(W).\Gamma_2(W) - D\,\Sigma\,\Psi_1(W) \\ \Gamma_3(W) = B\,\Sigma\,\Psi_2(W) + \frac{1}{12}B_2\,\Psi_1(W) - \frac{1}{6}\,B\,\mathrm{d}\Psi_1(W).\Gamma_1(W) \end{cases}$$

and it is also the case for the fourth-order terms:

(10) $$\begin{cases} \Psi_3(W) = \Sigma\,\mathrm{d}\Psi_1(W).\Gamma_2(W) + \mathrm{d}\Phi(W).\Gamma_3(W) - D\,\Sigma\,\Psi_2(W) + \Sigma\,\mathrm{d}\Psi_2(W).\Gamma_1(W) \\ \qquad + \frac{1}{6}\,D\,\mathrm{d}\Psi_1(W).\Gamma_1(W) - \frac{1}{12}\,D_2\,\Psi_1(W) - \frac{1}{12}\,\mathrm{d}\left(\mathrm{d}\Psi_1(W).\Gamma_1\right).\Gamma_1(W) \\ \Gamma_4(W) = B\,\Sigma\,\Psi_3(W) + \frac{1}{4}\,B_2\,\Psi_2(W) + \frac{1}{6}\,B\,D_2\,\Sigma\,\Psi_1(W) - \frac{1}{6}\,A\,B\,\Psi_2(W) \\ \qquad - \frac{1}{6}\,B\left(\mathrm{d}\left(\mathrm{d}\Phi.\Gamma_1\right).\Gamma_2(W) - \frac{1}{6}\,B\,\mathrm{d}\left(\mathrm{d}\Phi.\Gamma_2\right).\Gamma_1(W)\right) \\ \qquad - \frac{1}{6}\,B\,\Sigma\,\mathrm{d}\left(\mathrm{d}\Psi_1(W).\Gamma_1\right).\Gamma_1(W), \end{cases}$$

with

$$\begin{pmatrix} A_2 & B_2 \\ C_2 & D_2 \end{pmatrix} \equiv \begin{pmatrix} A & B \\ C & D \end{pmatrix}\begin{pmatrix} A & B \\ C & D \end{pmatrix} = \begin{pmatrix} A^2 + B\,C & A\,B + B\,D \\ C\,A + D\,C & C\,B + D^2 \end{pmatrix}.$$

In one spatial dimension, the previous A, B, C, D differential operators take a simpler form:

(11) $$A \equiv \overline{A}\,\partial_x\,,\ \ B \equiv \overline{B}\,\partial_x\,,\ \ C \equiv \overline{C}\,\partial_x\,,\ \ D \equiv \overline{D}\,\partial_x.$$

In the previous context, we introduce a nonuniform equilibrium:

(12) $$\Phi(W) \equiv E(x)\,W\,.$$

Then we can define a new nonhomogeneous differential operator δ with

(13) $$\delta W \equiv \partial_x\big(\Phi(W)\big) = \partial_x\big(E(x)\,W\big)\,.$$

We have $\delta = \frac{\partial E}{\partial x}\,\mathrm{I} + E(x)\,\partial_x$. Then we observe that the commutator $[\partial_x,\,\delta] \equiv \partial_x\,\delta - \delta\,\partial_x$ is not equal to zero: $[\partial_x,\,\delta]\,\varphi = \partial_x\,\partial_x(E(x)\,\varphi) - \partial_x(E(x)\,\partial_x\varphi) = \partial_x\big((\partial_x E)\,\varphi\big)$.

Proposition 3. Differential operators for linear nonuniform advection

In the previous context of a linear nonhomogeneous scheme, the differential operators Γ_1, Ψ_1, Γ_2, Ψ_2, Γ_3, Ψ_3 and Γ_4, defined at the relations (7)(9)(10), take the form

$$\Gamma_j \equiv \alpha_j\,W\,,\ \ \Psi_j \equiv \beta_j\,W$$

with the following algebraic relations

(14) $$\begin{cases} \alpha_1 = \overline{A}\,\partial_x + \overline{B}\,\delta \\ \beta_1 = E\,\alpha_1 - (\overline{C}\,\partial_x + \overline{D}\,\delta) \\ \alpha_2 = \overline{B}\,\Sigma\,\partial_x\,\beta_1 \\ \beta_2 = \Sigma\,\beta_1\,\alpha_1 + E\,\alpha_2 - \overline{D}\,\Sigma\,\partial_x\,\beta_1 \\ \alpha_3 = \overline{B}\,\Sigma\,\partial_x\,\beta_2 + \frac{1}{12}\,\overline{B_2}\,\partial_x^2\,\beta_1 - \frac{1}{6}\,\overline{B}\,\partial_x\,\beta_1\,\alpha_1 \\ \beta_3 = \Sigma\,\beta_1\,\alpha_2 + E\,\alpha_3 - \overline{D}\,\Sigma\,\partial_x\,\beta_2 + \Sigma\,\beta_2\,\alpha_1 + \frac{1}{6}\,\overline{D}\,\partial_x\,\beta_1\,\alpha_1 - \frac{1}{12}\,\beta_1\,\alpha_1^2 - \frac{1}{12}\,\overline{D_2}\,\partial_x^2\,\beta_1 \\ \alpha_4 = \overline{B}\,\Sigma\,\partial_x\,\beta_3 + \frac{1}{4}\,\overline{B_2}\,\partial_x^2\,\beta_2 + \frac{1}{6}\,\overline{B}\,\overline{D_2}\,\Sigma\,\partial_x^3\,\beta_1 - \frac{1}{6}\,\overline{A}\,\overline{B}\,\partial_x^2\,\beta_2 \\ \qquad - \frac{1}{6}\,\overline{B}\,\delta\,\alpha_1\,\alpha_2 - \frac{1}{6}\,\overline{B}\,\delta\,\alpha_2\,\alpha_1 - \frac{1}{6}\,\overline{B}\,\Sigma\,\partial_x\,\beta_1\,\alpha_1^2\,. \end{cases}$$

The proof of this proposition is a tedious algebraic calculation. It is presented in Annex A.

We consider in this contribution the case of the D1Q3 scheme with one conservation law with a cosine velocity field $u(x) \equiv \lambda U \cos(k\,x)$ introduced in (1). Then the differential operator δ proposed in (13) takes the form

$$\delta\varphi = \partial_x\big(E(x)\,\varphi\big) = \partial_x\left(\begin{array}{c}\lambda U \cos(k\,x)\varphi \\ \lambda^2\,\alpha\,\varphi\end{array}\right) = \partial_x\left(\begin{array}{c}u\,\varphi \\ \lambda^2\,\alpha\,\varphi\end{array}\right).$$

With the notation

(15) $$\partial_u\varphi \equiv U\,\partial_x\big(\cos(k\,x)\varphi\big)$$

if the velocity field is cosinusoidal (c.f. (1)) and

$$\partial_u\varphi \equiv U\,\partial_x\varphi$$

when the velocity field is constant, we have simply

(16) $$\delta = \left(\begin{array}{c}\lambda\,\partial_u \\ \lambda^2\,\alpha\,\partial_x\end{array}\right).$$

We observe that the differential operators ∂_x and ∂_u do not commute:

$$[\partial_x,\ \partial_u]\,\varphi = \partial_x\big(-k\,U\,\sin(k\,x)\,\varphi\big).$$

Proposition 4. D1Q3 differential operators for linear nonuniform advection
The linear differential operators explicited in (14) admit the following expressions in terms of the operators ∂_x and ∂_u. We have for the two first orders

(17) $$\alpha_1 = \lambda\,\partial_u,\ \beta_1 = \lambda^2\left(\begin{array}{c}\frac{u}{\lambda}\,\partial_u - \frac{\alpha+2}{3}\,\partial_x \\ \lambda\,(\alpha-1)\,\partial_u\end{array}\right)$$

(18) $$\left\{\begin{array}{l}\alpha_2 = \lambda^2\,\sigma\left(\partial_u^2 - \frac{\alpha+2}{3}\,\partial_x^2\right) \\ \beta_2 = \lambda^3\left(\begin{array}{c}2\,\sigma\,\frac{u}{\lambda}\,\partial_u^2 - \left(\frac{\alpha+2}{3}\,\sigma + \frac{\alpha-1}{3}\,\sigma'\right)\partial_x\,\partial_u - \frac{\alpha+2}{3}\,\sigma\,\frac{u}{\lambda}\,\partial_x^2 \\ \lambda\,(\alpha-1)\left((\sigma+\sigma')\,\partial_u^2 - \frac{\alpha+2}{3}\,\sigma\,\partial_x^2\right)\end{array}\right),\end{array}\right.$$

with the Hénon coefficients [17] σ and σ' defined according to

$$\sigma = \frac{1}{s} - \frac{1}{2},\ \sigma' = \frac{1}{s'} - \frac{1}{2}.$$

At third order, the formulae are more complicated. We have

(19) $$\alpha_3 = \lambda^3\left[\left(2\,\sigma^2 - \frac{1}{6}\right)\partial_u^3 + \left(\frac{\alpha+2}{3}\left(\frac{1}{6} - \sigma^2\right) + \frac{\alpha-1}{3}\left(\frac{1}{12} - \sigma\,\sigma'\right)\right)\partial_x^2\,\partial_u - \frac{\alpha+2}{3}\,\sigma^2\,\partial_u\,\partial_x^2\right]$$

and

$$\beta_3 \equiv \left(\begin{array}{c}\lambda^4\,\beta_{3J} \\ \lambda^5\,\beta_{3e}\end{array}\right),$$

with

(20) $$\left\{\begin{array}{l}\beta_{3J} = \frac{\alpha+2}{9}\left[-(1-\alpha)\,\sigma\,\sigma' + \left((\alpha+2)\,\sigma^2 + \frac{1}{4}\right)\right]\partial_x^3 \\ \quad + U\left[-2\,\frac{\alpha+2}{3}\,\sigma^2 + \frac{1-\alpha}{3}\,\sigma\,\sigma' + \frac{1+\alpha}{12}\right]\partial_x^2\,\partial_u - 2\,U\,\frac{\alpha+2}{3}\,\sigma^2\,\partial_u\,\partial_x^2 \\ \quad + \left[-2\,\frac{\alpha+2}{3}\,\sigma^2 + \frac{1-\alpha}{3}\left(2\,\sigma\,\sigma' + \sigma'^2 - \frac{1}{4}\right)\right]\partial_x\,\partial_u^2 + \left(5\,\sigma^2 - \frac{1}{4}\right)U\,\partial_u^3 \\ \beta_{3e} = \frac{1-\alpha}{3}\left[(\alpha+2)\,\sigma^2 + (1+2\,\alpha)\,\sigma\,\sigma' - \frac{1+\alpha}{4}\right]\partial_x^2\,\partial_u + (1-\alpha)\,\frac{\alpha+2}{3}\,\sigma\,(\sigma+\sigma')\,\partial_u\,\partial_x^2 \\ \quad - (1-\alpha)\left(2\,\sigma^2 + 2\,\sigma\,\sigma' + \sigma'^2 - \frac{1}{4}\right)\partial_u^3.\end{array}\right.$$

At fourth order, we have

$$(21) \quad \begin{cases} \alpha_4 = \lambda^4 \left[\frac{\alpha+2}{9} \left((\alpha+2)\,\sigma^3 - (1-\alpha)\,\sigma^2\,\sigma' - \frac{\alpha}{4}\,\sigma \right) \partial_x^4 \right. \\ \quad + \left[-2\frac{\alpha+2}{3}\,\sigma^3 + \frac{1-\alpha}{3}\left(2\,\sigma^2\,\sigma' + \sigma\,\sigma'^2 - \frac{1}{4}\,\sigma' \right) + \frac{1+2\,\alpha}{9}\,\sigma \right] \partial_x^2\,\partial_u^2 \\ \quad + \left[-2\frac{\alpha+2}{3}\,\sigma^3 + \frac{1-\alpha}{3}\,\sigma^2\,\sigma' + \frac{7+5\,\alpha}{36}\,\sigma \right] \partial_u\,\partial_x^2\,\partial_u \\ \quad \left. + \frac{\alpha+2}{3}\,\sigma\left(-2\,\sigma + \frac{1}{6} \right) \partial_u^2\,\partial_x^2 + \sigma\left(5\,\sigma^2 - \frac{3}{4} \right) \partial_u^4 \right]. \end{cases}$$

The proof of Proposition 4 is detailed in Annex B.

When the velocity field has a constant value $u(x) \equiv \lambda\,U$, super-convergence can be obtained with an appropriate choice of relaxation coefficients, called "magic" in [20]. Because magic is not science, we prefer the denomination of "quartic parameters" [12] to acheive fourth-order accuracy, or "cubic parameter" in the present case to obtain a third-order precision.

When the advection velocity field has a constant value, we have $\partial_u \equiv U\,\partial_x$ and the coefficient α_3 initially given according to (19) takes now the value

$$(22) \quad \alpha_3 = \frac{\lambda^3\,U}{12} \left[-2\,(1 - 12\,\sigma^2)\,U^2 + 4\,(1-\alpha)\,\sigma\,\sigma' + 1 + \alpha - 8\,(2+\alpha)\,\sigma^2 \right] \partial_x^3.$$

Then for a fixed set of values for U, α and σ, the cubic parameter σ'_c is defined by forcing to zero the value of α_3 in the relation (22):

$$(23) \quad \sigma'_c = \frac{2\,(1 - 12\,\sigma^2)\,U^2 + 8\,(2+\alpha)\,\sigma^2 - (1+\alpha)}{4\,(1-\alpha)\,\sigma}.$$

In the following, we first experiment with the D1Q3 lattice Boltzmann scheme with constant velocity, possibly with cubic parameters. Then we consider a cosine advection velocity. We detail in the next section the Fourier methodology developed to solve the various equivalent partial differential equations with very good precision.

5) Interlaced Fourier series

We compare the numerical simulation done with the D1Q3 lattice Boltzmann scheme with the solution of the equivalent partial differential equations up to fourth-order accuracy. This hierarchy of equations can be written

$$(24) \quad \frac{\partial\rho}{\partial t} + \sum_{j=1}^{\ell} \Delta t^{j-1}\,\alpha_j\,\rho = 0.$$

They are of order ℓ for $1 \leq \ell \leq 4$. We recall that we have the following structure

$$\begin{cases} \Delta t^0\,\alpha_1 = \lambda\,\partial_u \\ \Delta t^1\,\alpha_2 = -\mu\,\partial_x^2 + \mu_u\,\partial_u^2 \\ \Delta t^2\,\alpha_3 = \xi_u\,\partial_u^3 + \xi_{xu}\,\partial_x^2\,\partial_u + \xi_{ux}\,\partial_u\,\partial_x^2 \\ \Delta t^3\,\alpha_4 = \zeta_{u4}\,\partial_u^4 + \zeta_{xxuu}\,\partial_x^2\,\partial_u^2 + \zeta_{uxxu}\,\partial_u\,\partial_x^2\,\partial_u + \zeta_{uuxx}\,\partial_u^2\,\partial_x^2 + \zeta_{x4}\,\partial_x^4. \end{cases}$$

The coefficients μ, μ_u, ξ_u, ξ_{xu}, ξ_{ux}, ζ_{u4}, ζ_{xxuu}, ζ_{uxxu}, ζ_{uuxx} and ζ_{x4} are easy to explicate from the relations $(17)(18)(19)(21)$:

$$\begin{cases} \mu = \frac{\alpha+2}{3}\,\lambda^2\,\sigma\,, \ \mu_u = \lambda^2\,\sigma\,, \\ \xi_u = \lambda^3\left(2\,\sigma^2 - \frac{1}{6}\right),\ \xi_{xu} = \lambda^3\left(\frac{\alpha+2}{3}\left(\frac{1}{6} - \sigma^2\right) + \frac{\alpha-1}{3}\left(\frac{1}{12} - \sigma\,\sigma'\right)\right),\ \xi_{ux} = -\lambda^3\,\frac{\alpha+2}{3}\,\sigma^2 \\ \zeta_{u4} = \lambda^4\,\sigma\left(5\,\sigma^2 - \frac{3}{4}\right),\ \zeta_{xxuu} = \lambda^4\left[-2\,\frac{\alpha+2}{3}\,\sigma^3 + \frac{1-\alpha}{3}\left(2\,\sigma^2\,\sigma' + \sigma\,\sigma'^2 - \frac{1}{4}\,\sigma'\right) + \frac{1+2\alpha}{9}\,\sigma\right] \\ \zeta_{uxxu} = \lambda^4\left[-2\,\frac{\alpha+2}{3}\,\sigma^3 + \frac{1-\alpha}{3}\,\sigma^2\,\sigma' + \frac{7+5\,\alpha}{36}\,\sigma\right],\ \zeta_{uuxx} = \lambda^4\,\frac{\alpha+2}{3}\,\sigma\left(-2\,\sigma + \frac{1}{6}\right) \\ \zeta_{x4} = \lambda^4\left[\frac{\alpha+2}{9}\left((\alpha+2)\,\sigma^3 - (1-\alpha)\,\sigma^2\,\sigma' - \frac{\alpha}{4}\,\sigma\right)\right]. \end{cases}$$

We use a spectral method to capture an approximation of a partial differential equation of the family (24). In the case of an advective field given in (1), we introduce the two discrete spaces S_i and S_p defined as follows. The space of odd sine and even cosine is called S_i:

$$S_i \ni \rho = \sum_{j\geq 0} a_{2j+1}\,\sin\big((2j+1)\,k\,x\big) + \sum_{j\geq 0} a_{2j+2}\,\cos\big((2j+2)\,k\,x\big)$$

and the space of even sinus and odd cosinus is denoted by S_p:

$$S_p \ni \rho = \sum_{j\geq 0} b_{2j+1}\,\cos\big((2j+1)\,k\,x\big) + \sum_{j\geq 0} b_{2j+2}\,\sin\big((2j+2)\,k\,x\big).$$

The derivation operator breaks down into two parts:

$$\begin{cases} \partial_x^{ip}\ :\ S_i \longrightarrow S_p \\ \partial_x^{pi}\ :\ S_p \longrightarrow S_i\,. \end{cases}$$

Relatively to the basis $\big(\sin k\,x,\ \cos 2\,k\,x,\ \sin 3\,k\,x,\ \cos 4\,k\,x,\ \cdots\big)$ of S_i and to the basis $\big(\cos k\,x,\ \sin 2\,k\,x,\ \cos 3\,k\,x,\ \sin 4\,k\,x,\ \cdots\big)$ of S_p, the operators ∂_x^{ip} and ∂_x^{pi} admit the following matrices

$$\begin{cases} \Delta_x^{ip} = \mathrm{diag}\big(k,\ -2\,k,\ 3\,k,\ -4\,k,\ \cdots\big) \\ \Delta_x^{pi} = \mathrm{diag}\big(-k,\ 2\,k,\ -3\,k,\ 4\,k,\ \cdots\big) = -\Delta_x^{ip}. \end{cases}$$

The second order operator $\partial_x^2 = \partial_x^{pi} \circ \partial_x^{ip}$ operates inside the space S_i and is represented by the matrix

$$\Delta_x^{pi}\,\Delta_x^{ip} = -\mathrm{diag}\big(k^2,\ 4\,k^2,\ 9\,k^2,\ 16\,k^2,\ \cdots\big).$$

We introduce also the operator m_u of mutiplication by $u \equiv U\,\cos(k\,x)$. It operates from S_i and takes its values in S_p. Then $\partial_u = \partial_x \circ m_u$ operates inside the space S_i. More precisely, we have, without forgetting the constant component a_0:

$$m_u\,\rho = U\,\cos(k\,x)\left[a_0 + \textstyle\sum_{j\geq 0} a_{2j+1}\,\sin\big((2j+1)\,k\,x\big) + \sum_{j\geq 0} a_{2j+2}\,\cos\big((2j+2)\,k\,x\big)\right]$$
$$= \big(a_0 + \tfrac{1}{2}\,a_2\big)\,U\,\cos\big(k\,x\big) + \tfrac{U}{2}\,\textstyle\sum_{j\geq 0}\big(a_{2j+1} + a_{2j+3}\big)\,\sin\big((2j+2)\,k\,x\big)$$
$$+ \tfrac{U}{2}\,\textstyle\sum_{j\geq 1}\big(a_{2j} + a_{2j+2}\big)\,\cos\big((2j+1)\,k\,x\big).$$

The matrix

$$M_u \equiv \frac{U}{2}\begin{pmatrix} 0 & 1 & 0 & 0 \\ 1 & 0 & 1 & 0 \\ 0 & 1 & 0 & \ddots \\ 0 & 0 & \ddots & \ddots \end{pmatrix}$$

is a natural implementation of the operator m_u of multiplication by the velocity u for $\rho \in S_i$. Then the differential operator $\partial_u \equiv \partial_x\,m_u$ in the space S_i after truncation is represented by the matrix $\Delta_x^{pi}\,M_u$.

We have used two discretizations with 30 to 60 Fourier modes. After these algebraic operations, the partial differential equation (24) can be seen as an infinite system of ordinary differential equations

$$(25) \qquad \frac{\partial \rho}{\partial t} + A\,\rho = 0$$

with an operator A given at fourth order by the relation

$$(26) \quad \begin{cases} A = \lambda\, \partial_x\, m_u - \mu\, \partial_x^2 + \mu_u\, \partial_x\, m_u\, \partial_x\, m_u \\ \quad + \big(\xi_u\, \partial_x\, m_u\, \partial_x\, m_u\, \partial_x\, m_u + \xi_{xu}\, \partial_x^3\, m_u + \xi_{ux}\, \partial_x\, m_u\, \partial_x^2 \big) \\ \quad + \big(\zeta_{u4}\, \partial_x\, m_u\, \partial_x\, m_u\, \partial_x\, m_u\, \partial_x\, m_u + \zeta_{xxuu}\, \partial_x^3\, m_u\, \partial_x\, m_u + \zeta_{uxxu}\, \partial_x\, m_u\, \partial_x^3\, m_u \\ \quad + \zeta_{uuxx}\, \partial_x\, m_u\, \partial_x\, m_u\, \partial_x^2 + \zeta_{x4}\, \partial_x^4 \big)\,. \end{cases}$$

We observe that the matrix A is constant. Then after discretization with N modes, it becomes a constant matrix A_N. The system (25) is replaced by a system of a finite number of ordinary differential equations

$$(27) \qquad \frac{\partial \rho}{\partial t} + A_N\,\rho = 0\,.$$

Due to the fact that the matrix A_N is fixed, the solution of (27) is approached in this contribution by a Taylor expansion at order 5 from the initial condition ρ_0:

$$\rho(t) = \exp(-t\,A)\,\rho_0 \simeq \left[\mathrm{I} - t\,A + \frac{t^2}{2}\,A^2 - \frac{t^3}{6}\,A^3 + \frac{t^4}{24}\,A^4 - \frac{t^5}{120}\,A^5 \right] \rho_0\,.$$

In an initial series of numerical experiments, we have put in evidence approximations of the stationary solution of a lattice Boltzmann scheme forced with a cosine velocity field.

6)   Long-time asymptotic study with a cosine advection field

We have done numerical experiments with three advective velocities given by the relation (1) with $U = 0.0005$, $U = 0.005$ and $U = 0.05$. For each of these parameters, we have used four meshes with 64, 128, 256 et 512 points. We have made various choices for the approximation of the D1Q3 stationary field.

We first observe that the analytical expression of the stationary solution for the equation

$$\partial_t \rho + \partial_x \big(\lambda\,U\,\cos(k\,x)\,\rho \big) - \mu\, \partial_x^2 \rho = 0$$

with the integral condition

$$(28) \qquad \int_0^L \rho(x)\,\mathrm{d}x = 1.$$

can be explicated as

$$(29) \qquad \rho(x) = K\,\exp\left(\frac{\lambda\,U}{k\,\mu}\,\sin(k\,x) \right).$$

The normalization constant K in relation (29) is chosen such that the condition (28) is satisfied.

We compare the numerical solution obtained with the D1Q3 scheme with the numerical solution of Fourier series truncated with 30 active modes. We introduce an operator A obtained at various orders from the relation (26) typically and

$$A_\infty = \frac{1}{\partial_x} A.$$

Then $A_\infty \rho = \text{constant}$ and this constant is zero by periodicity of all the fonctions of the problem. Then $A_\infty \rho = 0$ with an operator A_∞ given at various orders by

$$A_\infty^1 = \lambda \, m_u - \mu \, \partial_x$$

at order 1,

$$A_\infty^2 = A_\infty^1 + \mu_u \, m_u \, \partial_x \, m_u$$

at order 2 and

$$A_\infty^3 = A_\infty^2 + \xi_u \, m_u \, \partial_x \, m_u \, \partial_x \, m_u + \xi_{xu} \, \partial_x^2 \, m_u + \xi_{ux} \, m_u \, \partial_x^2$$

at order 3 and finally,

$$\begin{cases} A_\infty^4 = A_\infty^3 + \zeta_{u4} \, m_u \, \partial_x \, m_u \, \partial_x \, m_u \, \partial_x \, m_u + \zeta_{xxuu} \, \partial_x^2 \, m_u \, \partial_x \, m_u + \zeta_{uxxu} \, m_u \, \partial_x^3 \, m_u \\ \qquad + \zeta_{uuxx} \, m_u \, \partial_x \, m_u \, \partial_x^2 + \zeta_{x4} \, \partial_x^3 \end{cases}$$

at order 4.

For $U = 0.0005$, the numerical results are presented in Figures 3a to 3d and the quantitative residuals in Table 1.
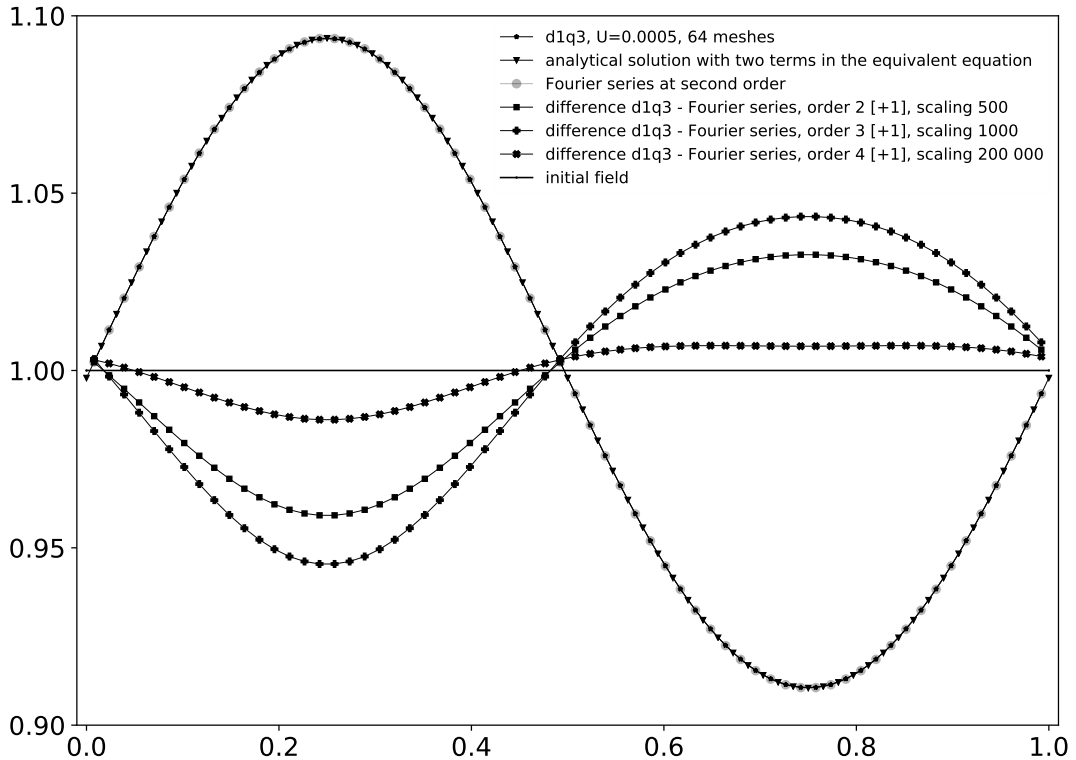
Figure 3a: Stationary field, $U = 0.0005$, 64 mesh points. Parameters of the D1Q3 scheme: $\alpha = -1$, $s = 1.5$, $s' = 1.2$. The symbol "[+1]" in the legend indicates that the value "+1" has been added to the data in order to display all curves in the same area of the graph. This convention is used in other graphs.
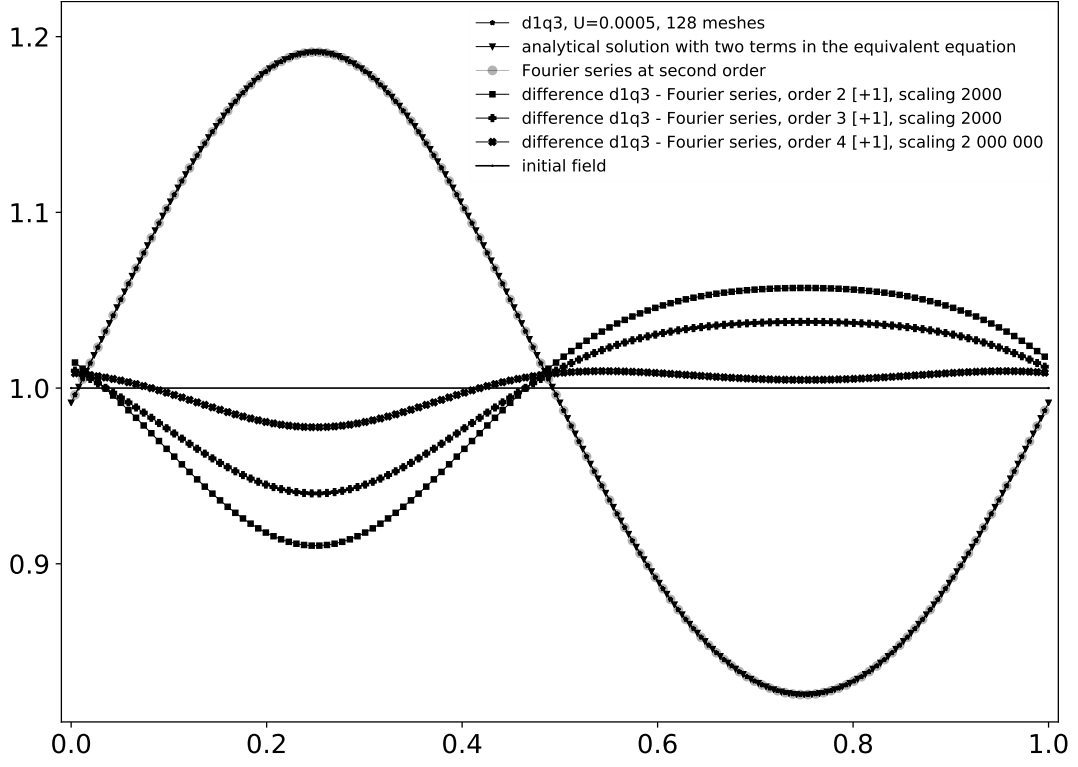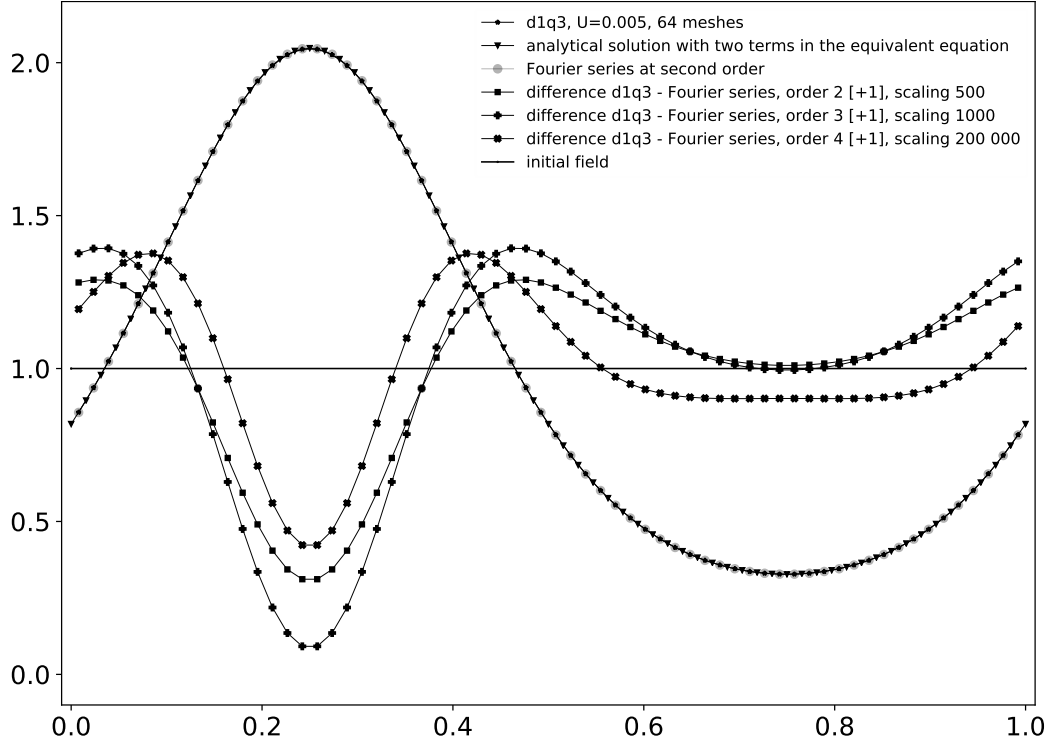
Figure 3b: Stationary field, $U = 0.0005$, 128 meshes.
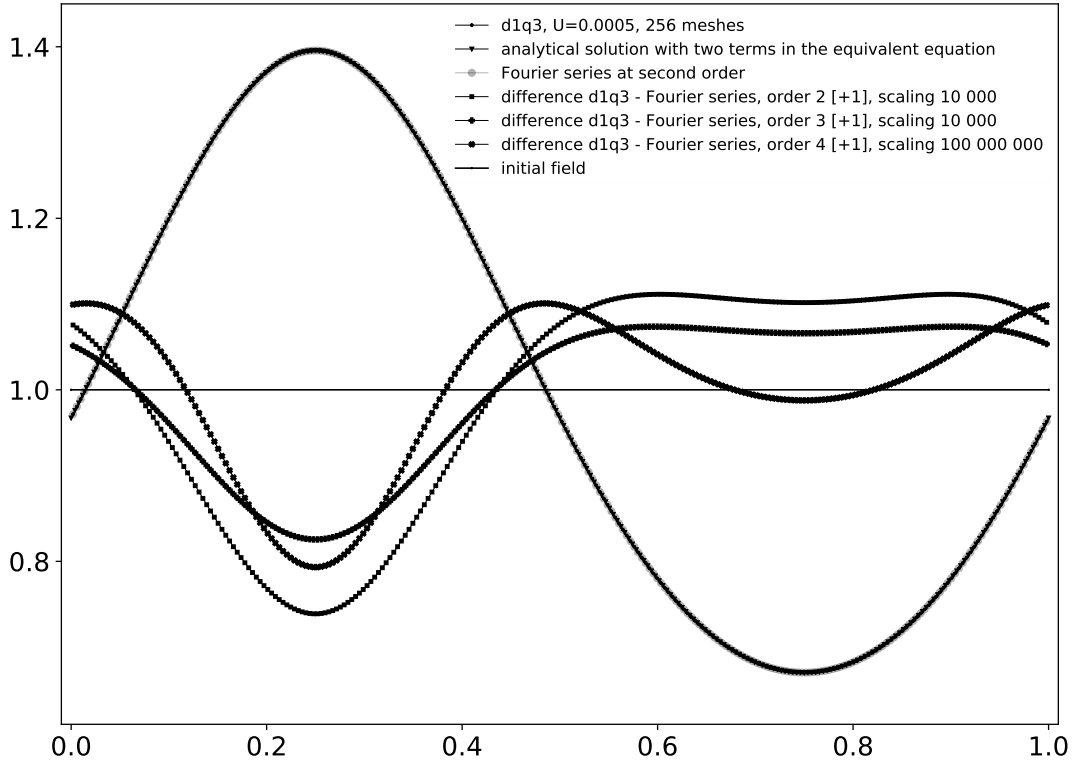
Figure 3c: Stationary field, $U = 0.0005$, 256 meshes.
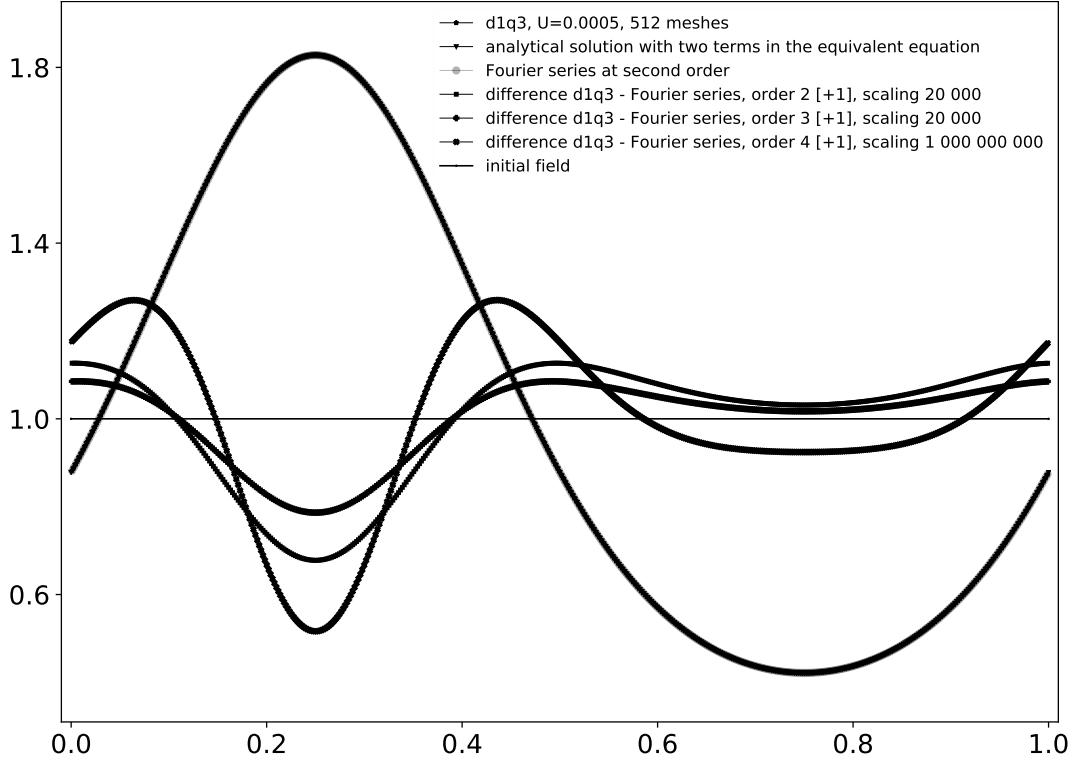
Figure 3d: Stationary field, $U = 0.0005$, 512 meshes.

mesh points \ equation order	1	2	3	4
64	$8.182\,10^{-5}$	$8.167\,10^{-5}$	$5.455\,10^{-5}$	$6.935\,10^{-8}$
128	$4.495\,10^{-5}$	$4.483\,10^{-5}$	$2.997\,10^{-5}$	$1.113\,10^{-8}$
256	$2.616\,10^{-5}$	$2.611\,10^{-5}$	$1.744\,10^{-5}$	$2.067\,10^{-9}$
512	$1.601\,10^{-5}$	$1.610\,10^{-5}$	$1.068\,10^{-5}$	$4.836\,10^{-10}$

Table 1: Differences between the lattice Boltzmann D1Q3 scheme and various equivalent equations for a stationary experiment with $U = 0.0005$

We observe that increasing precision improves the quality of the approximation between the lattice Boltzmann scheme and the computation with Fourier series. We observe that the discrete time needed to reach good precision can be very large. This is consistent with the relaxation diffusion time $\tau = \frac{\lambda}{\mu\,\Delta x\,k^2}$ measured with our scaling. For example, with 512 mesh points, we have used more than 3,400,000 time steps to reach the numerical result presented in Table 3. We observe also that the convergence order for the formal fourth-order approximation (fourth column of Table 1) is only 2.39.

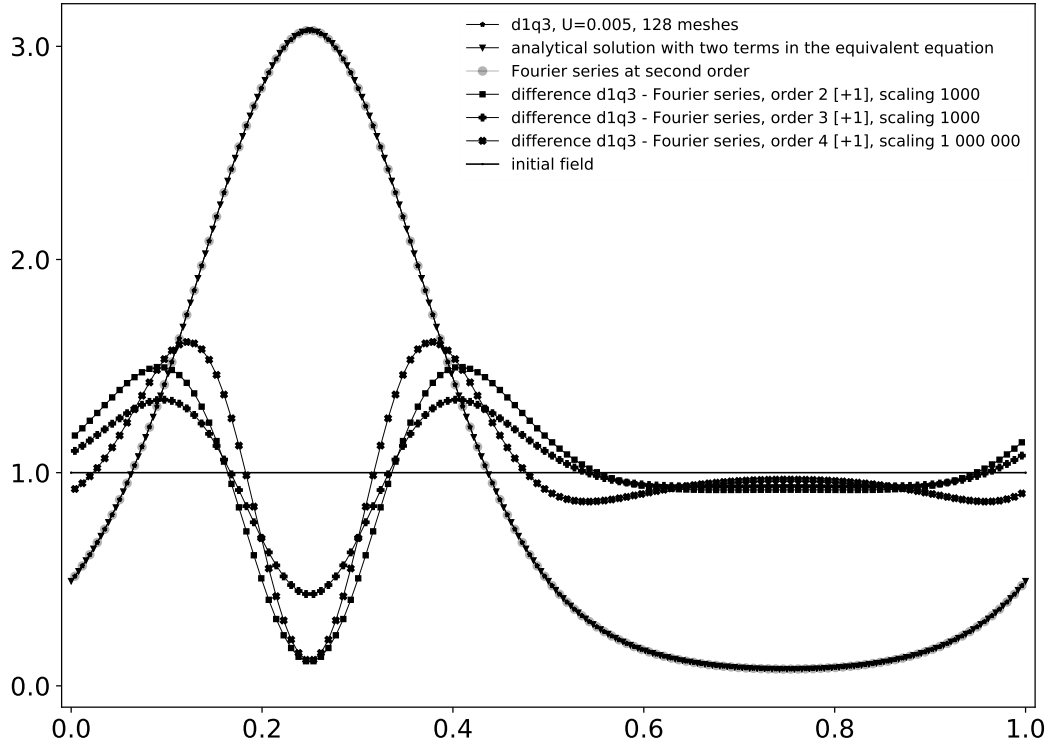Figure 4a: Stationary field, $U = 0.005$, 64 mesh points.

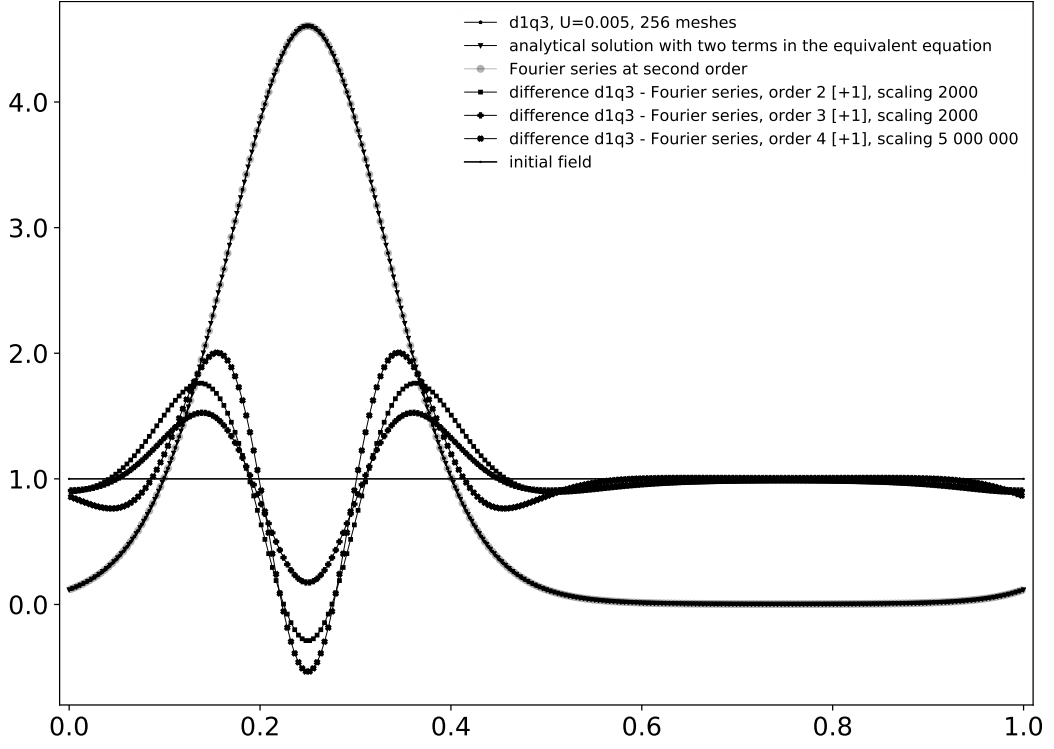Figure 4b: Stationary field, $U = 0.005$, 128 mesh points.

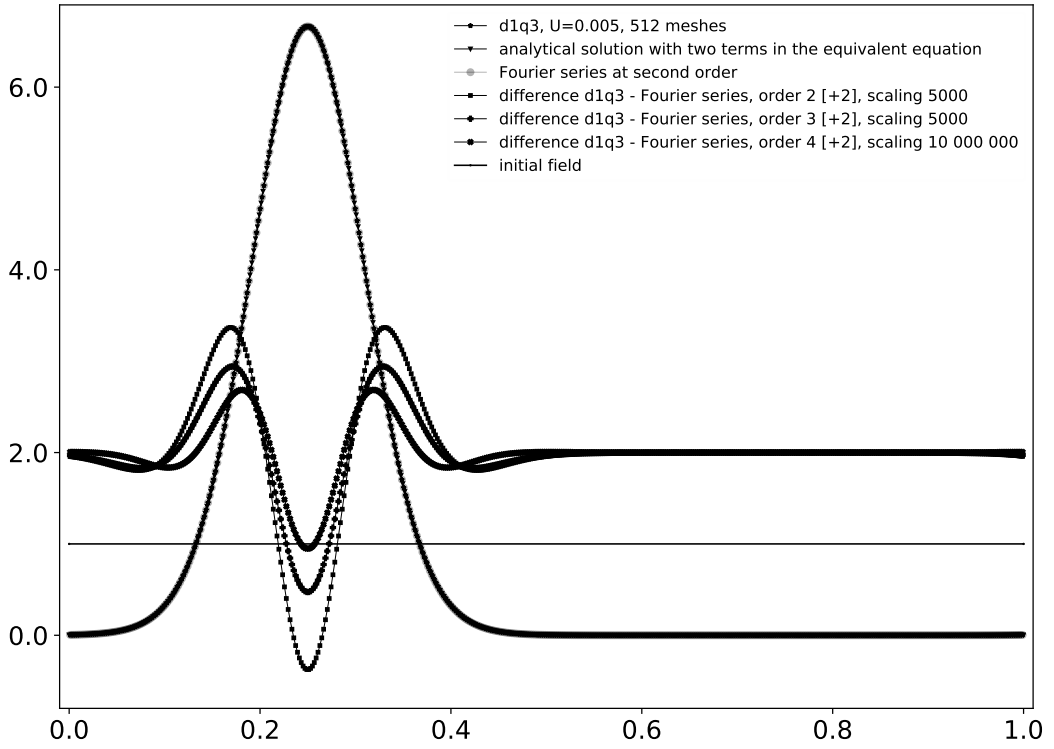Figure 4c: Stationary field, $U = 0.005$, 256 mesh points.

Figure 4d: Stationary field, $U = 0.005$, 512 mesh points.

For $U = 0.005$, we present the numerical results in Figures 4a to 4d and the quantitative residuals in Table 2. We again use 30 Fourier modes. The convergence process when the mesh is refined is slow. We have, for example, for the fourth-order partial differential equation (fourth column in Table 2), that a least-square fitting gives a convergence order of 1.58.

mesh points \ equation order	1	2	3	4
64	$1.350\,10^{-3}$	$1.378\,10^{-3}$	$9.083\,10^{-4}$	$2.886\,10^{-6}$
128	$8.538\,10^{-4}$	$8.845\,10^{-4}$	$5.692\,10^{-4}$	$8.780\,10^{-7}$
256	$6.183\,10^{-4}$	$6.437\,10^{-4}$	$4.122\,10^{-4}$	$3.066\,10^{-7}$
512	$4.578\,10^{-4}$	$4.750\,10^{-4}$	$3.052\,10^{-4}$	$1.052\,10^{-7}$

Table 2: Differences between the lattice Boltzmann D1Q3 scheme and various equivalent equations for a stationary experiment with $U = 0.005$

When $U = 0.05$, we have encountered a numerical difficulty. With 30 Fourier modes, the results are correct for 64 and 128 mesh points. But with 256 and 512 mesh points, oscillations appear in the numerical results. This is the sign of a under-resolved simulation. We have changed the number of Fourier modes and used 60 modes for 256 and 512 mesh points. We tested the representation of the solution of the D1Q3 scheme with a Fourier series. We have observed a residual in ℓ^∞ norm of $1.79\,10^{-14}$ and $6.06\,10^{-11}$. This precision is sufficient for our simulations. The results are presented in Figures 5a to 5d and in Table 3.
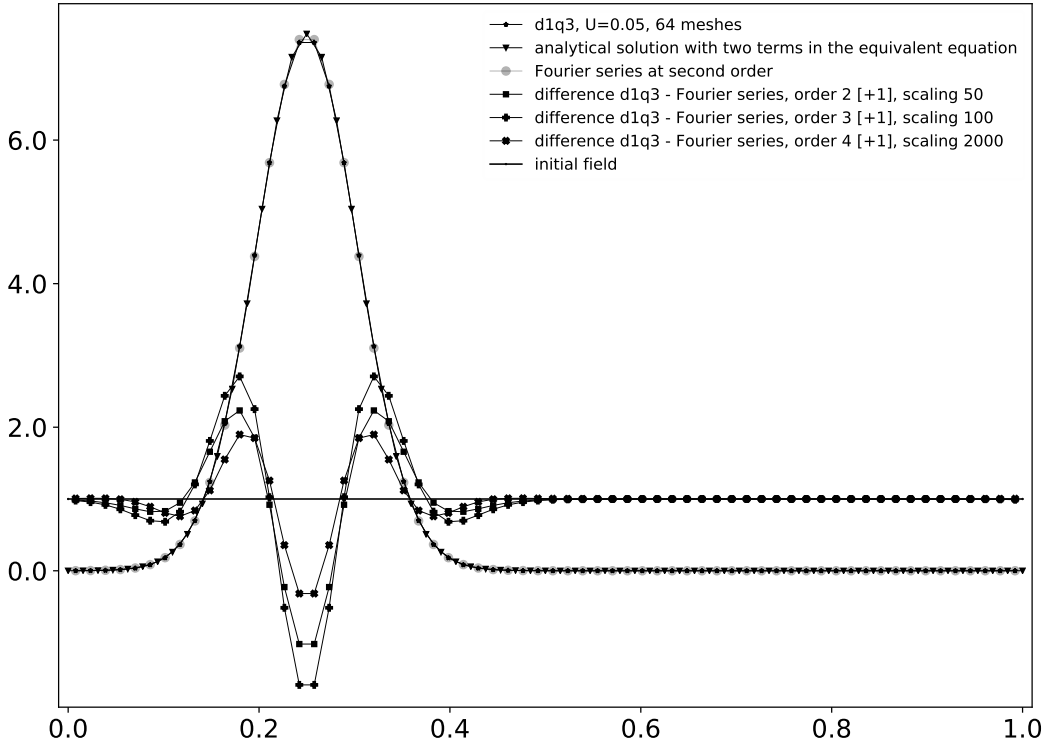

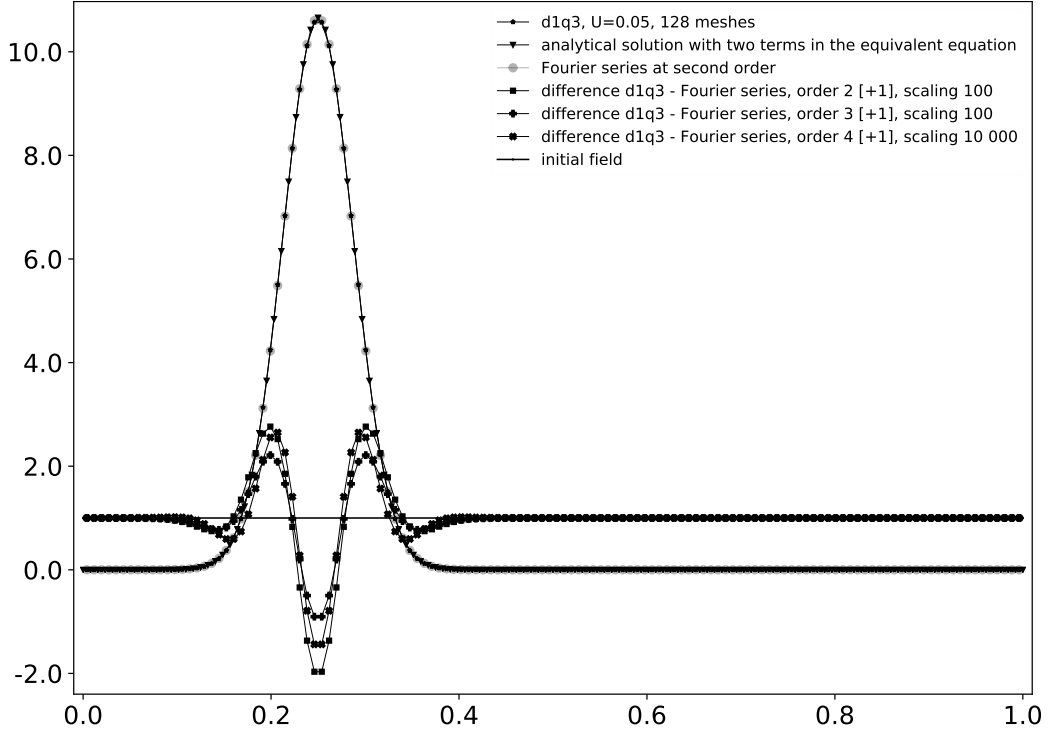Figure 5a: Stationary field, $U = 0.05$, 64 mesh points, 30 Fourier modes.

Figure 5b: Stationary field, $U = 0.05$, 128 mesh points, 30 Fourier modes.
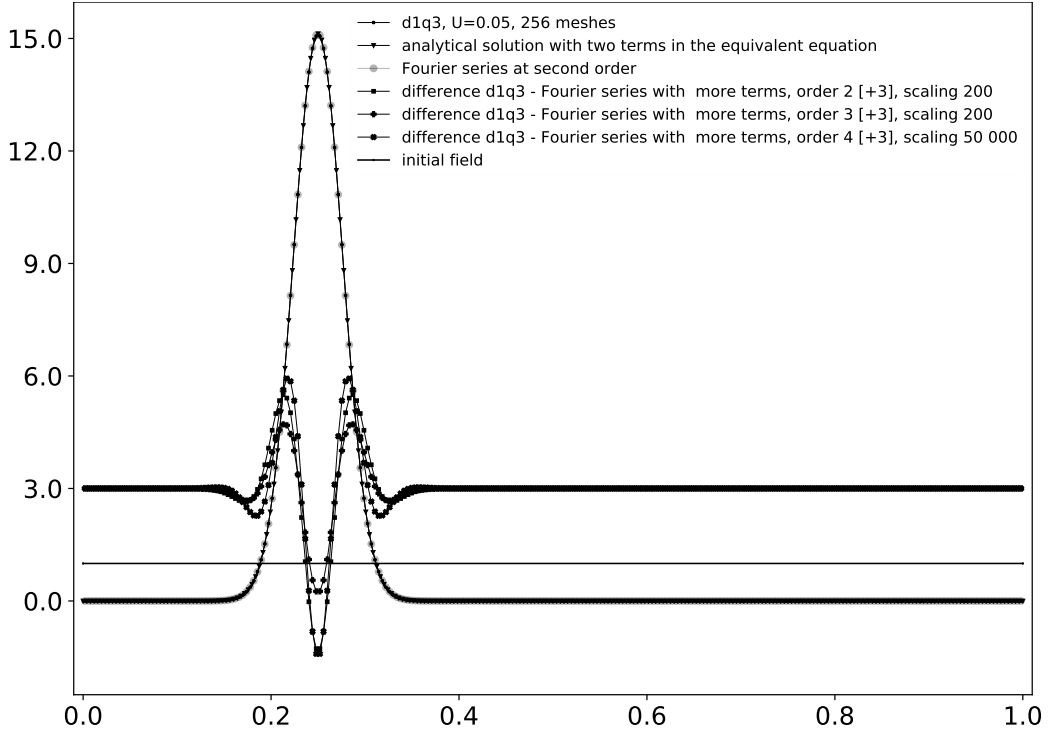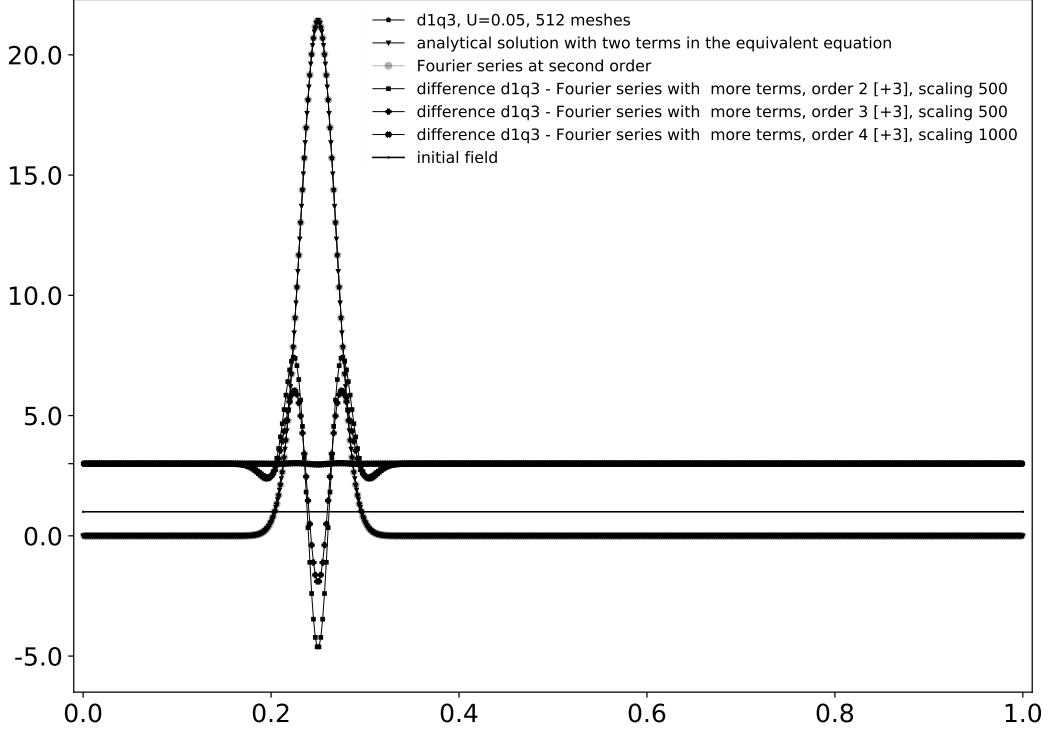

Figure 5c: Stationary field, $U = 0.05$, 256 mesh points, 60 Fourier modes.

Figure 5d: Stationary field, $U = 0.05$, 512 mesh points, 60 Fourier modes.

mesh points \ equation order	1	2	3	4
64	$3.883\,10^{-2}$	$4.042\,10^{-2}$	$2.590\,10^{-2}$	$6.585\,10^{-4}$
128	$2.856\,10^{-2}$	$2.967\,10^{-2}$	$1.904\,10^{-2}$	$2.439\,10^{-4}$
256	$2.057\,10^{-2}$	$2.136\,10^{-2}$	$1.372\,10^{-2}$	$8.820\,10^{-5}$
512	$1.468\,10^{-2}$	$1.523\,10^{-2}$	$9.790\,10^{-3}$	$3.153\,10^{-5}$

Table 3: Differences between the lattice Boltzmann D1Q3 scheme and various equivalent equations for a stationary experiment with $U = 0.05$

Once again, the order of convergence is not directly correlated with the order of the approximate partial differential equation. For example, the numerical order of convergence for the fourth-order partial differential equation is only 1.46.

We have also put in evidence some intrinsic properties of the D1Q3 lattice Boltzmann scheme with the first stationary mode. One step of the algorithm on a grid with N mesh points can be written

$$f(t + \Delta t) = A_{\mathrm{D1Q3}}\, f(t)$$

with A_{D1Q3} the global iteration matrix of order $3N \times 3N$ of this linear scheme. The matrix A_{D1Q3} contains all information relative to collision and advection for all the vertices. With an Arnoldi algorithm (see *e.g.* [22]), we extract the first eigenmode of the matrix A_{D1Q3}. This eigenvalue γ is numerically real in our case and we introduce a scaled parameter Γ

defined as follows. From the operator α_2 in (18), we first introduce the discrete equivalent viscosity $\kappa = \lambda \, \Delta x \, \sigma \, \frac{\alpha+2}{3}$. Then for a simulation with a wave number k, we set

$$(30) \qquad\qquad\qquad \Gamma = \frac{\gamma}{\kappa \, k^2}.$$

This is the scaled first eigenvalue of the iteration matrix $A_{\mathrm{D1}Q3}$. Then from the corresponding eigenvector f_γ, we extract the conserved moment

$$\rho_\gamma = \sum_{j=1}^{j=3} f_{\gamma, j}.$$

It is a function defined at all mesh points. We have represented in Figures 6-a to 6-d the corresponding modes for $U = 0$, 0.0005, 0.005 and 0.05. There is no simple correlation with the stationary results in Figures 3, 4 and 5 except for $U = 0.05$. In this case (Figure 6-d) the non-zero values of the mode concentrate in the left part of the interval $[0, \, L]$ as evidenced by the scale chosen for Figure 6-d.

The very interesting observation concerns the evolution of the eigenvalue Γ as function of velocity and number of mesh points ($N = 64$, 128, 356, 512) presented in Figure (7). A spectacular growth occurs for the largest velocity. In practice, the lattice Boltzmann scheme is much more viscous than proposed by the natural scaling $\kappa \, k^2$. This gives a first explanation of the large number of time steps (more than 3 million) necessary to reach convergence for the largest mesh in this case. We have also observed that for large values of the velocity U, we find values for Γ roughly proportional to $U \, N$.
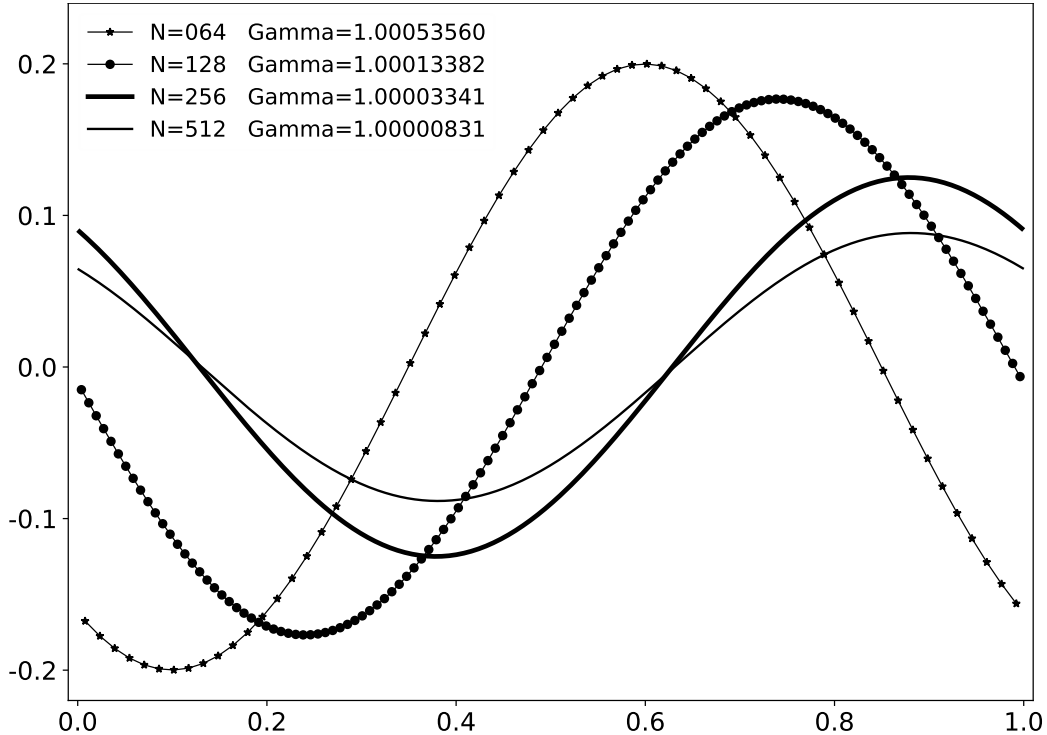

Figure 6-a: First eigenmode of the stationary D1Q3 discrete dynamics, $U = 0$.
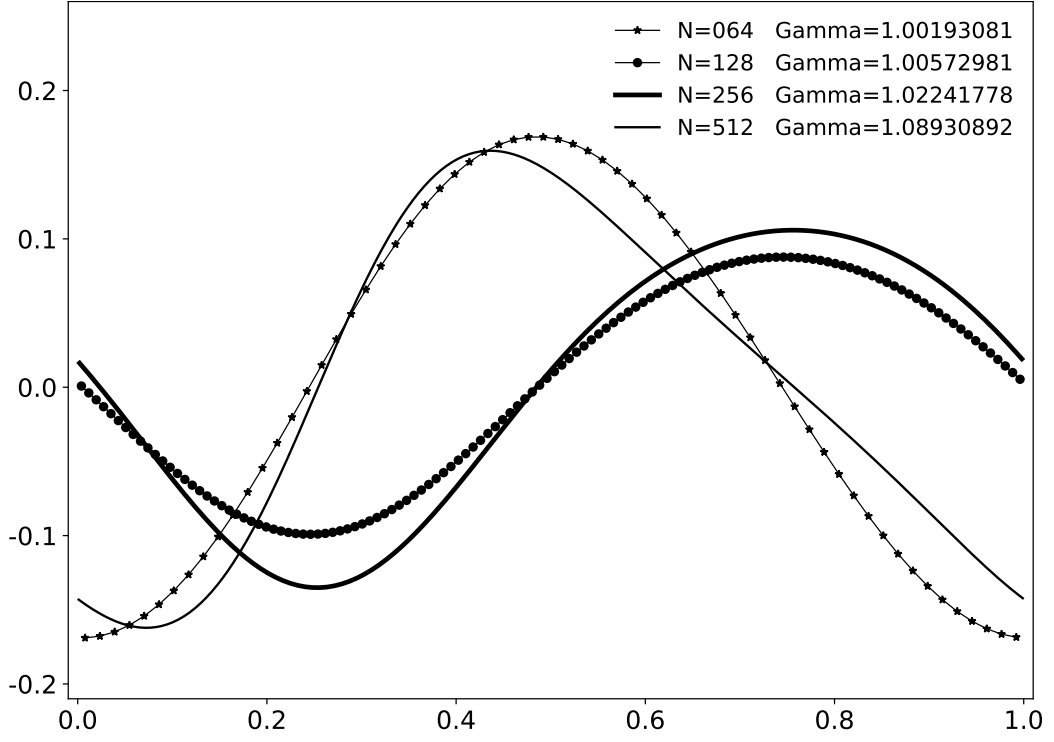
Figure 6-b: First eigenmode of the stationary D1Q3 discrete dynamics, $U = 0.0005$.
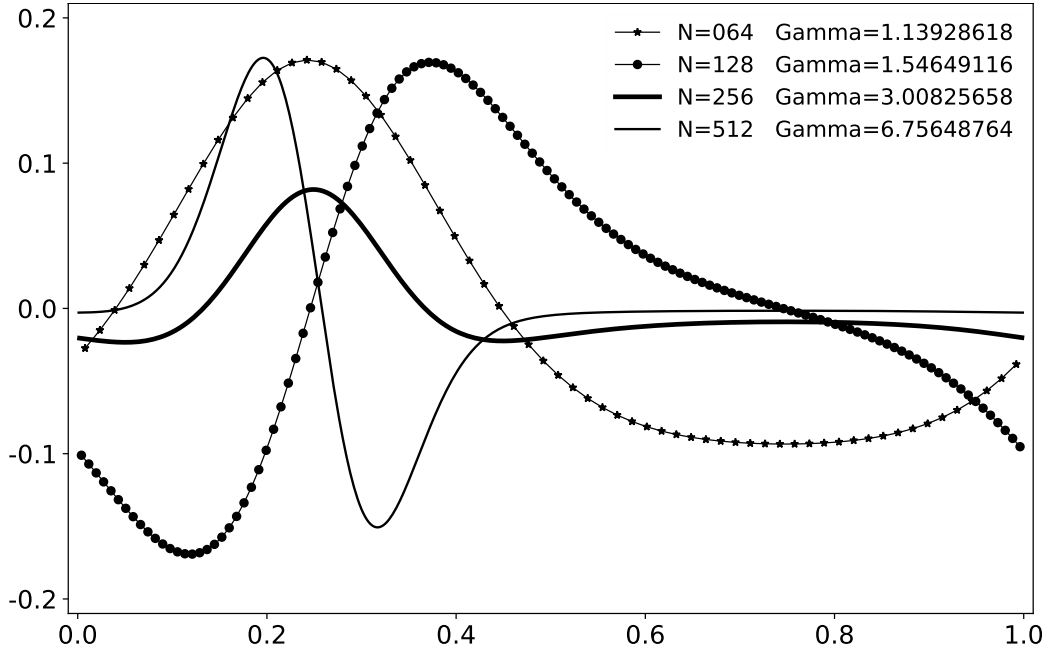

Figure 6-c: First eigenmode of the stationary D1Q3 discrete dynamics, $U = 0.005$.
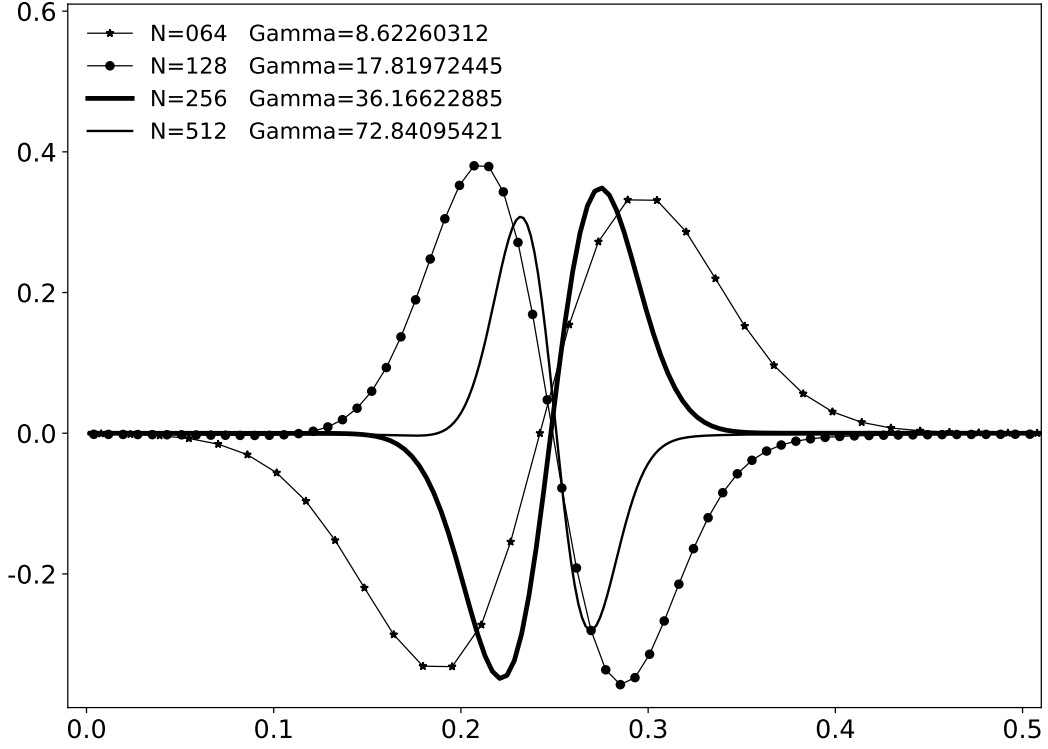
Figure 6-d: First eigenmode of the stationary D1Q3 discrete dynamics, $U = 0.05$.

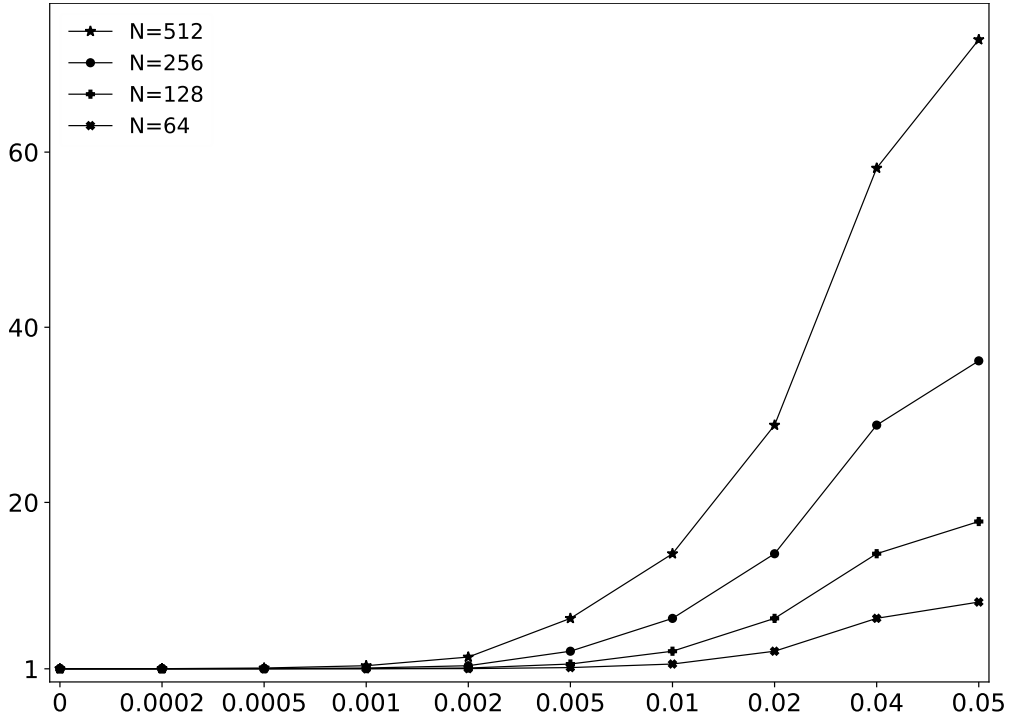Figure 7: First eigenvalue Γ defined in (30) for the stationary D1Q3 discrete dynamics as a function of velocity and number of mesh points. Observe that the x-scale is neither linear nor logarithmic to clearly highlight the numerical values.

As a partial conclusion for the stationary case, the analytic formula (29) obtained with the advective terms and only the uniform dissipation gives a very correct approximation of the stationary asymptotic solution obtained with the D1Q3 lattice Boltzmann scheme. It is just necessary to compute precisely the constant K in order to satisfy the integral condition (28). With higher-order Fourier series, the convergence is better. This experiment validates for nonuniform operators the formal expansion developed in the previous sections. Nevertheless, the speed of convergence towards the stationary state is not directly correlated with the order of the underlying partial differential equation.

7)   Unsteady evolution

We now compare the D1Q3 lattice Boltzmann scheme up to time $T = 1$ with the Fourier approximations of the various equivalent partial differential equations at various orders

$$\frac{\partial \rho}{\partial t} + A_j \, \rho = 0 \,, \ 1 \leq j \leq 4.$$

We have at order 1:

$$A_1 = \lambda \, \partial_x \, m_u \,,$$

at order 2:

$$A_2 = A_1 - \mu \, \partial_x^2 + \mu_u \, \partial_x \, m_u \, \partial_x \, m_u \,,$$

at order 3:

$$A_3 = A_2 + \left(\xi_u \, \partial_x \, m_u \, \partial_x \, m_u \, \partial_x \, m_u + \xi_{xu} \, \partial_x^3 \, m_u + \xi_{ux} \, \partial_x \, m_u \, \partial_x^2 \right) ,$$

and at order 4:

$$\begin{cases} A_4 = A_3 + \left(\zeta_{u4} \, \partial_x \, m_u \, \partial_x \, m_u \, \partial_x \, m_u \, \partial_x \, m_u + \zeta_{xxuu} \, \partial_x^3 \, m_u \, \partial_x \, m_u \right. \\ \qquad \left. + \zeta_{uxxu} \, \partial_x \, m_u \, \partial_x^3 \, m_u + \zeta_{uuxx} \, \partial_x \, m_u \, \partial_x \, m_u \, \partial_x^2 + \zeta_{x4} \, \partial_x^4 \right) . \end{cases}$$

We have chosen the following parameters

$$U = 0.005 \,, \ \alpha = -1 \,, \ \sigma = 0.01 \ [s = 1.960784313725] \,, \ s' = 1.2$$

with $\sigma \equiv \frac{1}{s} - \frac{1}{2}$. The results are presented in a triple series of two figures for $N = 64$ and $N = 128$ mesh points respectively. In Figures 8a and 8b, we consider a constant velocity field with a sinusoidal initial condition. In Figures 9a and 9b, a cosine velocity field with a sinusoidal initial condition is studied. Finally the Figures 10a and 10b present the case of a cosine advection field with a constant initial field ($\rho_0 \equiv 1$). These figures show that the approximation of the lattice Boltzmann scheme with the equivalent partial differential equations is globally correct. Then we refine the mesh up to $N = 1024$ points. The results are presented in Figure 11. They are not completely satisfactory.
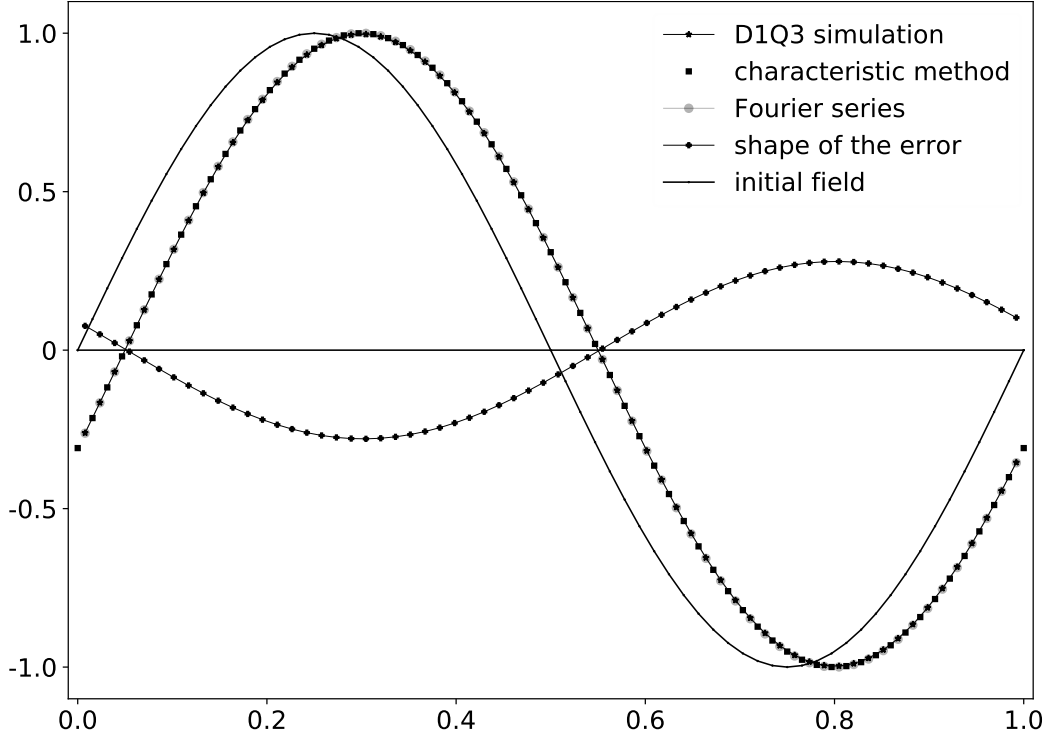
Figure 8a: Unsteady evolution, constant advection field [$U = 0.05$], 64 mesh points, sinusoidal initial condition.
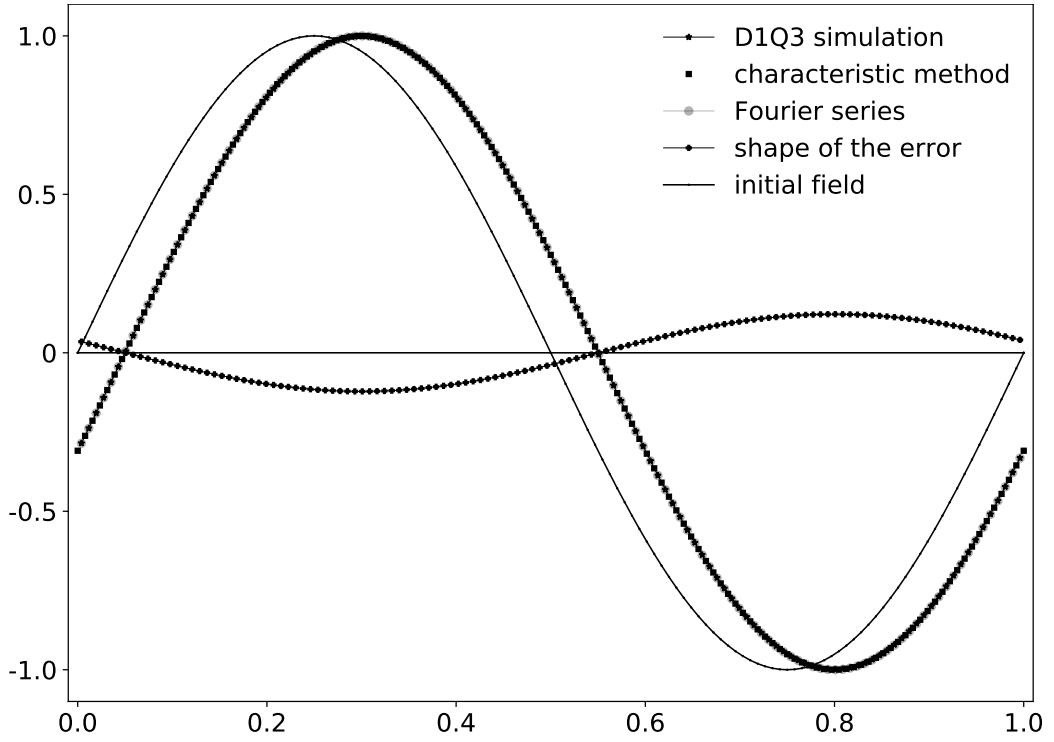

Figure 8b: Unsteady evolution, constant advection field [$U = 0.05$], 128 mesh points, sinusoidal initial condition.

Figure 9a: Unsteady evolution, sinusoidal advection field [$U = 0.05$], 64 mesh points, sinusoidal initial condition.
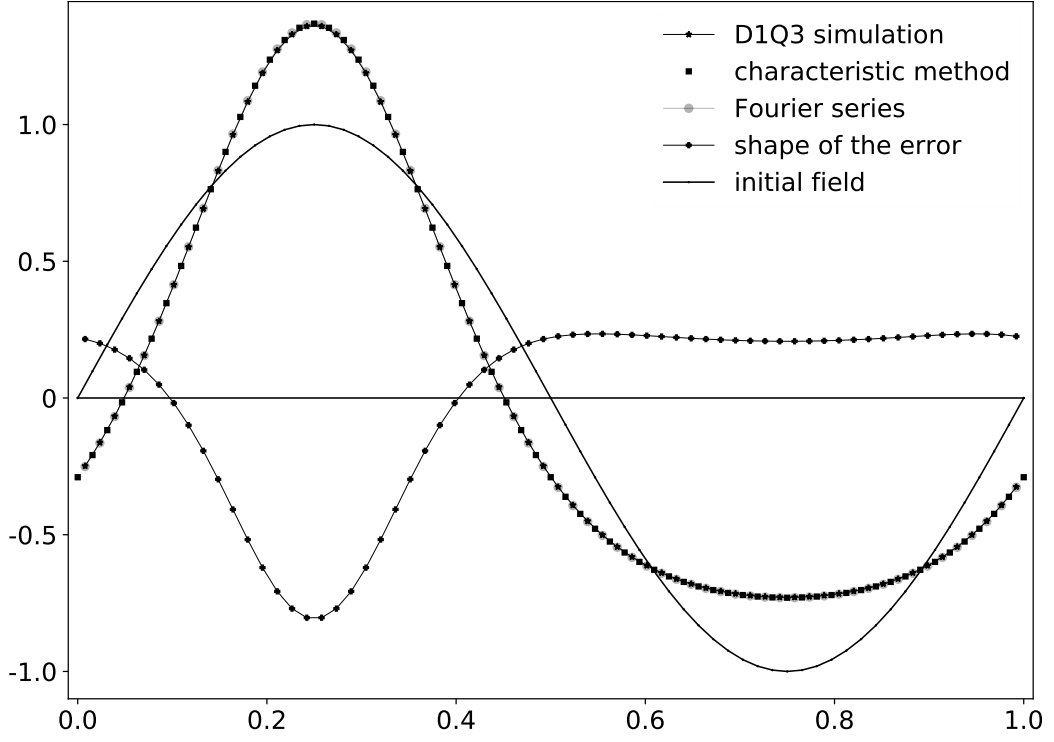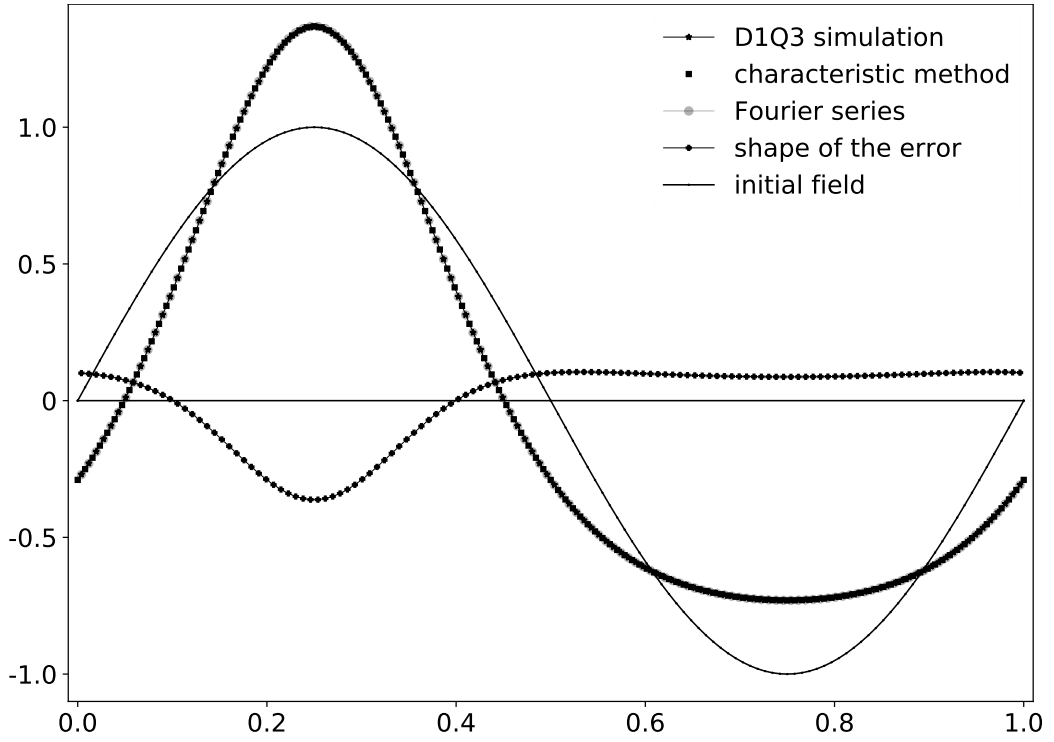

Figure 9b: Unsteady evolution, sinusoidal advection field [$U = 0.05$], 128 mesh points, sinusoidal initial condition.
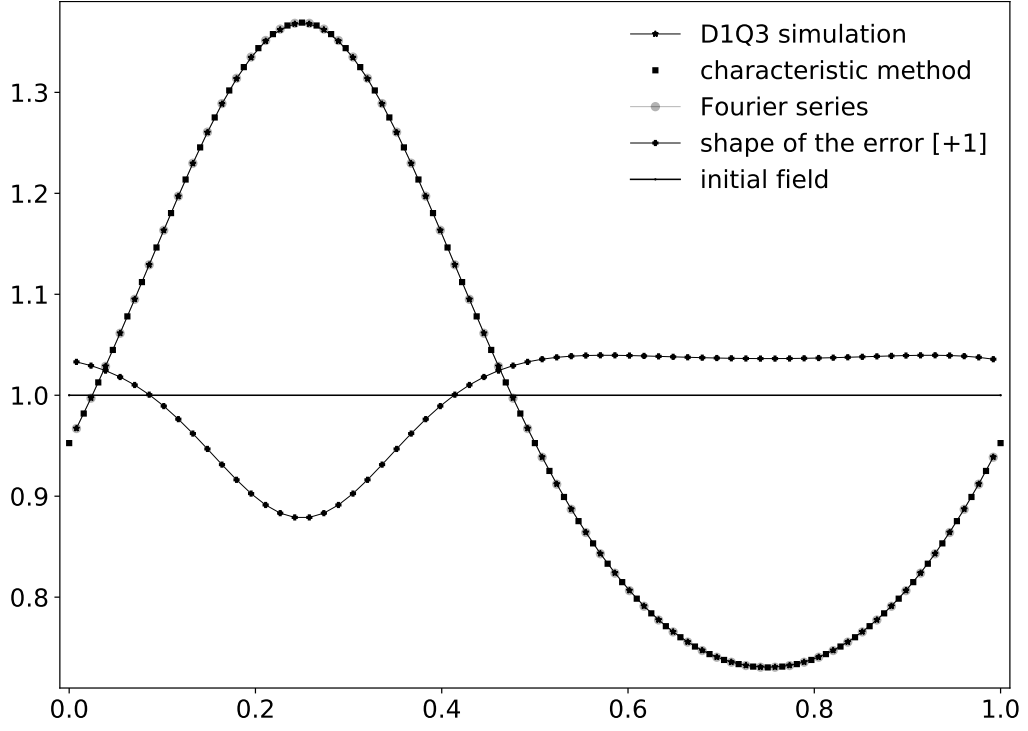
Figure 10a: Unsteady evolution, sinusoidal advection field $[U = 0.05]$, 64 mesh points, constant initial condition.
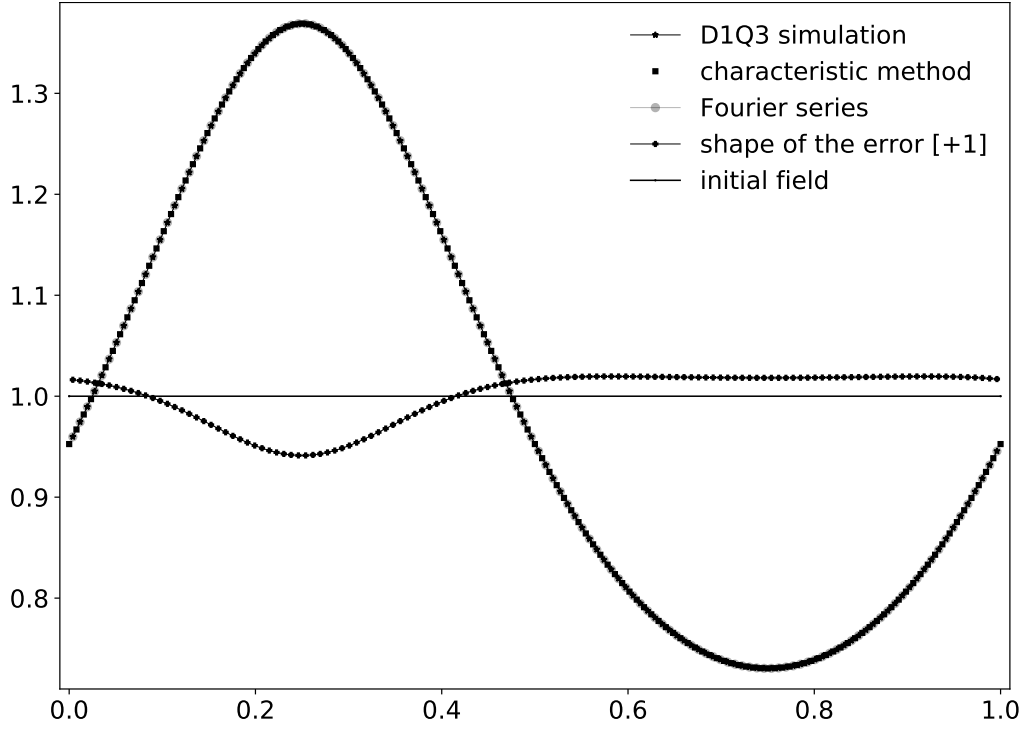

Figure 10b: Unsteady evolution, sinusoidal advection field $[U = 0.05]$, 128 mesh points, constant initial condition.
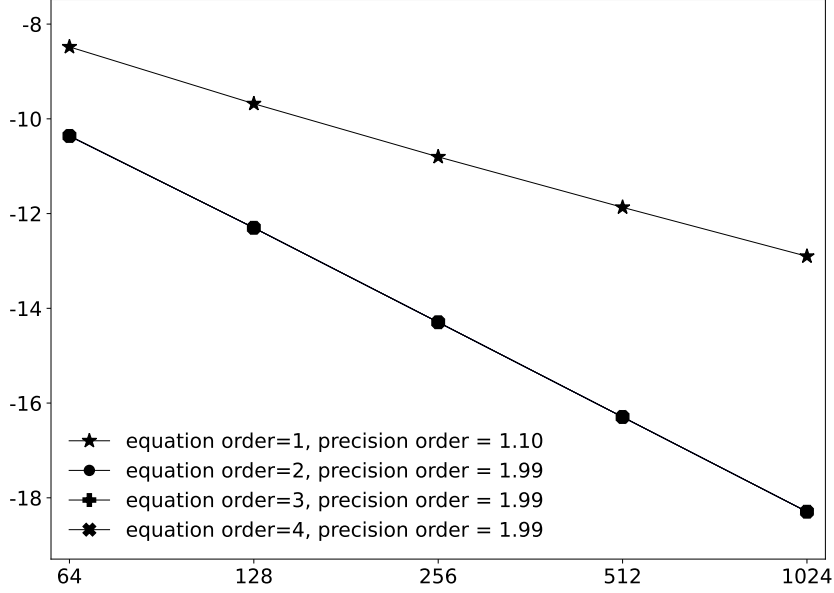
Figure 11: Errors measured with the maximum norm between the D1Q3 lattice Boltzmann scheme [with parameters $\alpha = -1$, $\sigma \equiv \frac{1}{s} - \frac{1}{2} = 0.01$, $s' = 1.2$] and various equivalent partial differential equations for an unsteady experiment with constant velocity field $U = 0.05$, finite-time evolution with final time $T = 1$, and initialization with a sine wave. The x-axis represents the number of mesh points with a logarithmic scale and the y-axis is graduated with the base-2 logarithm of the error. The microscopic moments were initialized with the equilibrium values.

In order to overcome the moderate speed of convergence for an unsteady evolution, we focus in the next section on the way the lattice Boltzmann scheme is initialized.

8)   Initialization of microscopic moments

In the previous section, we have taken the non-conserved moments at time $t = 0$ equal to the value at equilibrium:

$$(31) \qquad\qquad\qquad\qquad Y_0(t = 0) = \Phi(\rho_0).$$

We recall the asymptotic expansion of nonconserved moments for a lattice Boltzmann scheme through the general expression (8):

$$Y = \Phi(W) + S^{-1} \left(\Delta t \, \Psi_1(W) + \Delta t^2 \, \Psi_2(W) \right) + \mathrm{O}(\Delta t^3).$$

For the advective D1Q3 scheme with a cosine advection field,

$$Y = \begin{pmatrix} j \\ e \end{pmatrix} , \ \Phi(\rho) = \begin{pmatrix} \lambda \, U \, \cos(k\,x)\,\rho \\ \lambda^2 \, \alpha \, \rho \end{pmatrix} , \ \Psi_1 = \beta_1\,\rho , \ \beta_1 = \lambda^2 \begin{pmatrix} u\,\partial_u - \frac{\alpha+2}{3}\,\partial_x \\ \lambda\,(\alpha - 1)\,\partial_u \end{pmatrix}$$

and

$$\Psi_2 = \beta_2\,\rho , \ \beta_2 = \lambda^3 \begin{pmatrix} 2\,\sigma\,\frac{u}{\lambda}\,\partial_u^2 - \left(\frac{\alpha+2}{3}\,\sigma + \frac{\alpha-1}{3}\,\sigma'\right)\partial_x\,\partial_u - \frac{\alpha+2}{3}\,\sigma\,\frac{u}{\lambda}\,\partial_x^2 \\ \lambda\,(\alpha - 1)\left((\sigma + \sigma')\,\partial_u^2 - \frac{\alpha+2}{3}\,\sigma\,\partial_x^2\right) \end{pmatrix} .$$

27

For initialization at order 0, the relation (31) is simply applied. The initialization suggested by Mei, Luo, Lallemand and d'Humières [24] at order 1 is:

$$(32) \qquad\qquad Y_1(t = 0) = \Phi(\rho_0) + \Delta t \, S^{-1} \, \beta_1 \, \rho_0.$$

In the following, we also consider a second-order initialization:

$$(33) \qquad\qquad Y_2(t = 0) = \Phi(\rho_0) + S^{-1} \left(\Delta t \, \beta_1 \, \rho_0 + \Delta t^2 \, \beta_2 \, \rho_0 \right).$$

We remark that this framework can certainly be revisited with the new version of lattice Boltzmann schemes through multistep finite difference schemes, as proposed by Bellotti, Graille and Massot [3]. The results of our simulations are presented in the next section.

9)   Unsteady fields for a constant or variable advective velocity

We first study the uniform advection case. Then we specify the case of cubic parameters. Then we look to nonuniform cosine advection. In all cases, the choice of the initialization scheme has a great influence on the final precision. Observe also that only one mode is needed for the Fourier approximation when the velocity advection is constant.

mesh points \ equation order	1	2	3	4
initialization order	0	0	0	0
64	$2.798 \; 10^{-3}$	$7.606 \; 10^{-4}$	$7.604 \; 10^{-4}$	$7.596 \; 10^{-4}$
128	$1.218 \; 10^{-3}$	$1.983 \; 10^{-4}$	$1.983 \; 10^{-4}$	$1.982 \; 10^{-4}$
256	$5.598 \; 10^{-4}$	$4.979 \; 10^{-5}$	$4.979 \; 10^{-5}$	$4.978 \; 10^{-5}$
512	$2.675 \; 10^{-4}$	$1.245 \; 10^{-5}$	$1.245 \; 10^{-5}$	$1.245 \; 10^{-5}$
1024	$1.307 \; 10^{-4}$	$3.113 \; 10^{-6}$	$3.112 \; 10^{-6}$	$3.112 \; 10^{-6}$
convergence order	1.10	1.99	1.99	1.99

Table 4: Errors measured with the maximum norm between the D1Q3 lattice Boltzmann scheme [with parameters $\alpha = -1$, $\sigma \equiv \frac{1}{s} - \frac{1}{2} = 0.01$, $s' = 1.2$] and various equivalent partial differential equations for an unsteady experiment: constant velocity field $U = 0.05$, finite time evolution with final time $T = 1$, and initialization with a sinus wave. The error remains second-order accurate even if we use the third-order or the fourth-order equivalent equation for the approximation of the lattice Boltzmann scheme. Figure 11 is an other representation of these results.

With the first-order initialization (32), the results are presented in Figure 12 and Table 5. They become consistent for the three first levels of approximation, but there is no convergence at fourth-order accuracy.
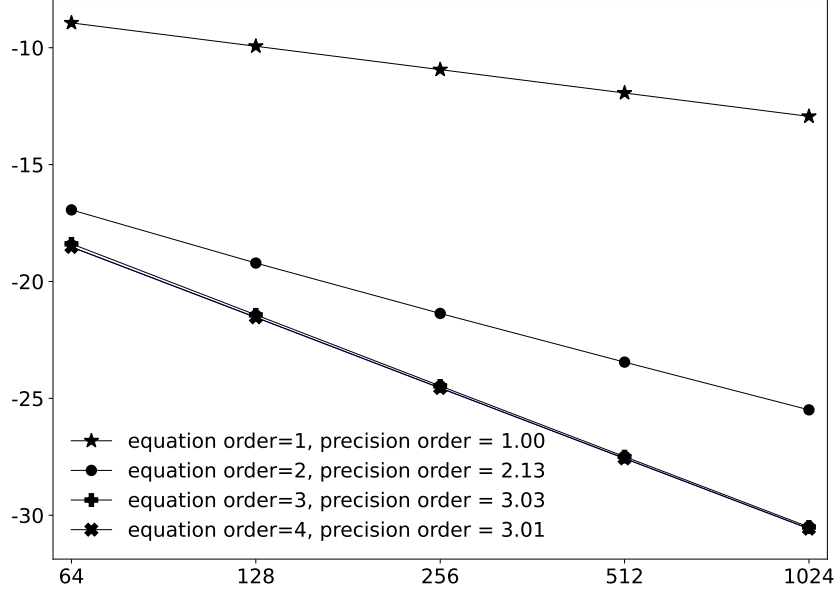
Figure 12: Same experiment as the one described in Figure 11 with the initialization of the microscopic moments at first order following (32).

mesh points \ equation order	1	2	3	4
initialization order	1	1	1	1
64	$2.039\ 10^{-3}$	$7.967\ 10^{-6}$	$2.911\ 10^{-6}$	$2.652\ 10^{-6}$
128	$1.020\ 10^{-3}$	$1.648\ 10^{-6}$	$3.544\ 10^{-7}$	$3.290\ 10^{-7}$
256	$5.101\ 10^{-4}$	$3.697\ 10^{-7}$	$4.305\ 10^{-8}$	$4.049\ 10^{-8}$
512	$2.551\ 10^{-4}$	$8.730\ 10^{-8}$	$5.296\ 10^{-9}$	$5.018\ 10^{-9}$
1024	$1.275\ 10^{-4}$	$2.120\ 10^{-8}$	$6.569\ 10^{-10}$	$6.247\ 10^{-10}$
convergence order	1.00	2.13	3.03	3.01

Table 5: Same numerical experiment as the one described in Table 4, except that the initialization has been changed to the first-order approximation (32). The precision is improved for second order and we obtain the third order correctly, but the fourth-order approximation is only converging up to third order.

With the second-order initialization (33), the results are displayed in Figure 13 and Table 6. The experimental order of approximation is now coherent up to fourth order. In Table 7, economical initialization orders are used to present an optimal convergence accuracy.
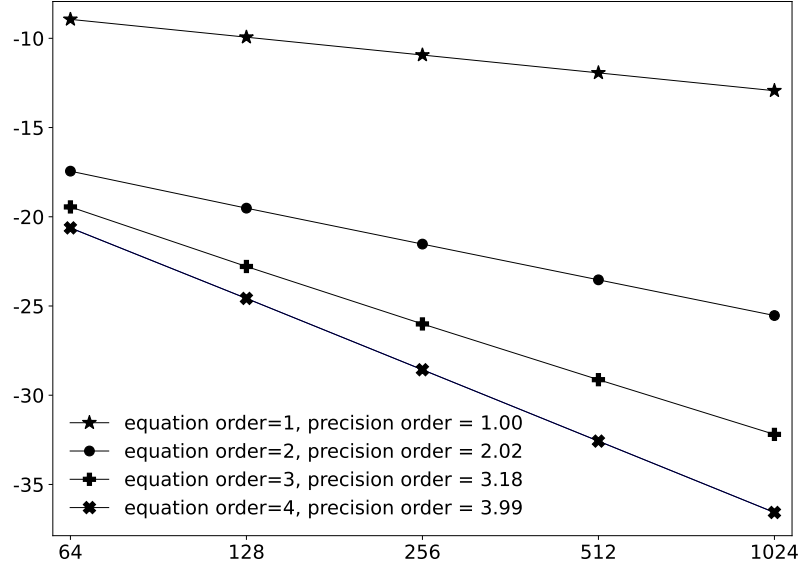
Figure 13: Same experiment as the one described in Figure 11, with the initialization of the microscopic moments at second order following (33).

mesh points \ equation order	1	2	3	4
initialization order	2	2	2	2
64	$2.039 \ 10^{-3}$	$5.607 \ 10^{-6}$	$1.397 \ 10^{-6}$	$6.191 \ 10^{-7}$
128	$1.020 \ 10^{-3}$	$1.332 \ 10^{-6}$	$1.382 \ 10^{-7}$	$3.997 \ 10^{-8}$
256	$5.101 \ 10^{-4}$	$3.299 \ 10^{-7}$	$1.485 \ 10^{-8}$	$2.506 \ 10^{-9}$
512	$2.551 \ 10^{-4}$	$8.233 \ 10^{-8}$	$1.703 \ 10^{-9}$	$1.567 \ 10^{-10}$
1024	$1.275 \ 10^{-4}$	$2.057 \ 10^{-8}$	$2.034 \ 10^{-10}$	$9.798 \ 10^{-12}$
convergence order	1.00	2.02	3.18	3.99

Table 6: Same numerical experiment as the one described in Table 4, except that the initialization has been changed to the second-order approximation (33). The precision order is now consistent with the approximation order.

mesh points \ equation order	1	2	3	4
initialization order	0	0	1	2
64	$2.798 \ 10^{-3}$	$7.606 \ 10^{-4}$	$2.911 \ 10^{-6}$	$6.191 \ 10^{-7}$
128	$1.218 \ 10^{-3}$	$1.983 \ 10^{-4}$	$3.544 \ 10^{-7}$	$3.997 \ 10^{-8}$
256	$5.598 \ 10^{-4}$	$4.979 \ 10^{-5}$	$4.305 \ 10^{-8}$	$2.506 \ 10^{-9}$
512	$2.675 \ 10^{-4}$	$1.245 \ 10^{-5}$	$5.296 \ 10^{-9}$	$1.567 \ 10^{-10}$
1024	$1.307 \ 10^{-4}$	$3.113 \ 10^{-6}$	$6.569 \ 10^{-10}$	$9.798 \ 10^{-12}$
convergence order	1.10	1.99	3.03	3.99

Table 7: Optimal initialization orders for the numerical experiment described in Table 4. The precision order is now consistent with the approximation order without any extra calculus for the initialization at the lowest orders.

In a second series of experiments with a constant velocity field, we use cubic parameters:

$$U = 0.05\,, \ \alpha = -1\,, \ \sigma = 0.01\,,$$

as previously. The second relaxation coefficient s' such that the relation (23) is satisfied:

$$\sigma' = 0.072425\,, \ s' = 1.7469537493994847$$

with $\sigma' \equiv \frac{1}{s'} - \frac{1}{2}$. The initial condition is still a sine wave and we need only one term in the Fourier series.

In Table 8, the initialization for the second-order approximation is only of order zero and the cubic convergence property is not obtained. On the other hand, when the initialization for the second-order partial differential equation is first order accurate (see Table 9), the second-order and third-order approximations are identical.

mesh points \ equation order	1	2	3	4
initialization order	0	0	1	2
64	$2.826 \ 10^{-3}$	$7.882 \ 10^{-4}$	$2.181 \ 10^{-6}$	$6.455 \ 10^{-7}$
128	$1.219 \ 10^{-3}$	$1.988 \ 10^{-4}$	$2.332 \ 10^{-7}$	$4.063 \ 10^{-8}$
256	$5.598 \ 10^{-4}$	$4.980 \ 10^{-5}$	$2.665 \ 10^{-8}$	$2.544 \ 10^{-9}$
512	$2.675 \ 10^{-4}$	$1.245 \ 10^{-5}$	$3.174 \ 10^{-9}$	$1.590 \ 10^{-10}$
1024	$1.307 \ 10^{-4}$	$3.113 \ 10^{-6}$	$3.869 \ 10^{-10}$	$9.951 \ 10^{-12}$
convergence order	1.11	2.00	3.11	4.00

Table 8: Errors measured with the maximum norm between the D1Q3 lattice Boltzmann scheme with cubic parameters $\alpha = -1$, $\sigma \equiv \frac{1}{s} - \frac{1}{2} = 0.01$ ($s = 1.96078$), $\sigma' = 0.072425$ ($s' = 1.74695$) for the unsteady experiment described in the caption of Table 4. Even if the relaxation parameters have been fitted in order to obtain third-order accuracy with the second-order equivalent partial differential equation, the error remains second-order accurate in this case.

mesh points \ equation order	1	2	3	4
initialization order	0	1	1	2
64	$2.826 \ 10^{-3}$	$2.181 \ 10^{-6}$	$2.181 \ 10^{-6}$	$6.455 \ 10^{-7}$
128	$1.219 \ 10^{-3}$	$2.332 \ 10^{-7}$	$2.332 \ 10^{-7}$	$4.063 \ 10^{-8}$
256	$5.598 \ 10^{-4}$	$2.665 \ 10^{-8}$	$2.665 \ 10^{-8}$	$2.544 \ 10^{-9}$
512	$2.675 \ 10^{-4}$	$3.174 \ 10^{-9}$	$3.174 \ 10^{-9}$	$1.590 \ 10^{-10}$
1024	$1.307 \ 10^{-4}$	$3.869 \ 10^{-10}$	$3.869 \ 10^{-10}$	$9.951 \ 10^{-12}$
convergence order	1.11	3.11	3.11	4.00

Table 9: Same numerical experiment as the one described in Table 8, except that the initialization scheme is first-order accurate when comparing with the second-order equivalent partial differential equation. The third-order terms of the partial differential equation are identically null in this case due to the choice of a set of cubic parameters, and the order of accuracy jumps to third order.

When the velocity is no longer constant but given by the relation (1), the modes are coupled as detailed in Section 5. We have used 30 active modes in the Fourier series. In Tables 10 to 12, we experiment with the three types of initialization, (31), (32) and (33). The results are qualitatively identical to the previous experiments with a uniform vector field. When the initialization is done with the equilibrium (31), the lattice Boltzmann scheme can be compared with equivalent partial differential equations only at second order, as detailed in Table 10. For the first order (32), third-order accuracy can be obtained. Nevertheles, the fourth-order differential model is only third-order accurate (Table 11). With a second-order initialization (33), the asymptotic partial differential equation of a given degree is an approximation of the lattice Boltzmann scheme with the same degree, as presented in Table 12.

mesh points \ equation order	1	2	3	4
initialization order	0	0	0	0
64	$5.625 \ 10^{-3}$	$1.172 \ 10^{-3}$	$1.120 \ 10^{-3}$	$1.088 \ 10^{-3}$
128	$2.534 \ 10^{-3}$	$2.952 \ 10^{-4}$	$2.819 \ 10^{-4}$	$2.778 \ 10^{-4}$
256	$1.195 \ 10^{-3}$	$7.327 \ 10^{-5}$	$6.992 \ 10^{-5}$	$6.940 \ 10^{-5}$
512	$5.793 \ 10^{-4}$	$1.823 \ 10^{-5}$	$1.739 \ 10^{-5}$	$1.733 \ 10^{-5}$
1024	$2.851 \ 10^{-4}$	$4.547 \ 10^{-6}$	$4.337 \ 10^{-6}$	$4.329 \ 10^{-6}$
convergence order	1.07	2.00	2.00	2.00

Table 10: Same numerical experiment as the one described in Table 4; the uniform vector field is replaced by a cosine velocity (1). As in the previous experiment, the error remains second-order accurate even if we use the third-order or the fourth-order equivalent equation for the approximation of the lattice Boltzmann scheme.

mesh points \ equation order	1	2	3	4
initialization order	1	1	1	1
64	$4.561 \ 10^{-3}$	$1.087 \ 10^{-4}$	$5.628 \ 10^{-5}$	$2.446 \ 10^{-5}$
128	$2.259 \ 10^{-3}$	$1.982 \ 10^{-5}$	$6.495 \ 10^{-6}$	$2.427 \ 10^{-6}$
256	$1.126 \ 10^{-3}$	$4.124 \ 10^{-6}$	$7.747 \ 10^{-7}$	$2.622 \ 10^{-7}$
512	$5.620 \ 10^{-4}$	$9.336 \ 10^{-7}$	$9.441 \ 10^{-8}$	$3.018 \ 10^{-8}$
1024	$2.808 \ 10^{-4}$	$2.216 \ 10^{-7}$	$1.165 \ 10^{-8}$	$3.610 \ 10^{-9}$
convergence order	1.01	2.23	3.06	3.18

Table 11: Same numerical experiment as the one described in Table 10. The initialization is now given by the first-order approximation (32). The precision is improved for the second-order partial differential equation and we obtain the third-order correctly. But the fourth-order approximation is converging only up to third order.

mesh points \ equation order	1	2	3	4
initialization order	2	2	2	2
64	$4.548 \ 10^{-3}$	$9.505 \ 10^{-5}$	$4.264 \ 10^{-5}$	$1.082 \ 10^{-5}$
128	$2.257 \ 10^{-3}$	$1.807 \ 10^{-5}$	$4.742 \ 10^{-6}$	$6.741 \ 10^{-7}$
256	$1.125 \ 10^{-3}$	$3.904 \ 10^{-6}$	$5.540 \ 10^{-7}$	$4.162 \ 10^{-8}$
512	$5.620 \ 10^{-4}$	$9.060 \ 10^{-7}$	$6.678 \ 10^{-8}$	$2.544 \ 10^{-9}$
1024	$2.808 \ 10^{-4}$	$2.182 \ 10^{-7}$	$8.191 \ 10^{-9}$	$1.522 \ 10^{-10}$
convergence order	1.00	2.19	3.08	4.03

Table 12: Same numerical experiment as the one described in Table 10. The initialization is now given by the second order approximation (33). The precision order is now consistent with the approximation order.

Optimal initialization orders for the numerical experiment with sinusoidal velocity can be made precise as follows:

$$
\begin{cases}
\text{partial differential equation order} & = 1 \text{ or } 2: & \text{initialization at order } 0 \\
\text{partial differential equation order} & = 3: & \text{initialization at order } 1 \\
\text{partial differential equation order} & = 4: & \text{initialization at order } 2.
\end{cases}
$$

The precision order is now consistent with the approximation order without any extra calculus for the initialization at the lowest orders.

If the initial condition is no longer a sinus wave but a constant state, the results presented in Tables 10 to 12 are essentially unchanged. We present in Table 13 the analogue of Table 8 for this case.

mesh points \ equation order	1	2	3	4
initialization order	0	0	1	2
64	$6.050 \ 10^{-4}$	$3.597 \ 10^{-5}$	$1.224 \ 10^{-5}$	$1.306 \ 10^{-6}$
128	$2.932 \ 10^{-4}$	$7.528 \ 10^{-6}$	$1.475 \ 10^{-6}$	$8.102 \ 10^{-8}$
256	$1.447 \ 10^{-4}$	$1.699 \ 10^{-6}$	$1.800 \ 10^{-7}$	$5.034 \ 10^{-9}$
512	$7.194 \ 10^{-5}$	$4.024 \ 10^{-7}$	$2.221 \ 10^{-8}$	$3.130 \ 10^{-10}$
1024	$3.587 \ 10^{-5}$	$9.784 \ 10^{-8}$	$2.758 \ 10^{-9}$	$1.943 \ 10^{-11}$
convergence order	1.02	2.13	3.03	4.01

Table 13: Optimal initialization orders for the numerical experiment with sinusoidal velocity described in Table 10. The initial condition is changed from a sinusoidal function to a constant state, as shown in Figures 10a and 10b. Each asymptotic partial differential equation presents a precision order consistent with its approximation order.

We tried also to apply a cubic choice of coefficients for the non homogeneous case. We have not observed any spectacular improved precision. There is no inconsistency because the cubic parameters have been explicated with the hypothesis of a constant velocity field.

10) Conclusion

In this contribution, we have extended the ABCD asymptotic analysis developed in [9] and [10] to a nonhomogeneous linear problem. It has been necessary to develop a small library of Fourier series to approximate with high accuracy the equivalent partial differential equations at orders 1 to 4. The differential operators have been explicated with the help of formal calculation and, in particular, the Sagemath [29] library.

For a stationary problem after a long time evolution, we have not observed a complete consistency between the lattice Boltzmann scheme and the four differential models. The models are asymptotically correct but the order of accuracy is not the one suggested by the order of the partial differential equation. A first explanation is the fact that the asymptotic model is derived for space-time evolution and not for purely stationary problems. This question could be specifically studied in a future work.

The main result concerns a finite-time evolution. We have put in evidence the importance of a correct initialization order to force the Boltzmann scheme to simulate a partial differential equation at high order. This question could be naturally revisited within the framework introduced by Bellotti *et al.* in [3].

It would be useful to consider in the future a two-dimensional situation to get information about anisotropic defects of lattice Boltzmann schemes.

Acknowledgments

Annex A. Proof of Proposition 3

We first recall the general result presented in [9] and [10]. We have

$$(34) \begin{cases} \Gamma_1(W) = A\,W + B\,\Phi(W) \\ \Psi_1(W) = \mathrm{d}\Phi(W).\Gamma_1(W) - \big(C\,W + D\,\Phi(W)\big) \\ \Gamma_2(W) = B\,\Sigma\,\Psi_1(W) \\ \Psi_2(W) = \Sigma\,\mathrm{d}\Psi_1(W).\Gamma_1(W) + \mathrm{d}\Phi(W).\Gamma_2(W) - D\,\Sigma\,\Psi_1(W) \\ \Gamma_3(W) = B\,\Sigma\,\Psi_2(W) + \frac{1}{12}B_2\,\Psi_1(W) - \frac{1}{6}B\,\mathrm{d}\Psi_1(W).\Gamma_1(W) \\ \Psi_3(W) = \Sigma\,\mathrm{d}\Psi_1(W).\Gamma_2(W) + \mathrm{d}\Phi(W).\Gamma_3(W) - D\,\Sigma\,\Psi_2(W) + \Sigma\,\mathrm{d}\Psi_2(W).\Gamma_1(W) \\ \qquad + \frac{1}{6}D\,\mathrm{d}\Psi_1(W).\Gamma_1(W) - \frac{1}{12}D_2\,\Psi_1(W) - \frac{1}{12}\mathrm{d}\big(\mathrm{d}\Psi_1(W).\Gamma_1(W)\big).\Gamma_1(W) \\ \Gamma_4(W) = B\,\Sigma\,\Psi_3(W) + \frac{1}{4}B_2\,\Psi_2(W) + \frac{1}{6}B\,D_2\,\Sigma\,\Psi_1(W) - \frac{1}{6}A\,B\,\Psi_2(W) \\ \qquad - \frac{1}{6}B\,\mathrm{d}\,(\mathrm{d}\Phi.\Gamma_1).\Gamma_2(W) - \frac{1}{6}B\,\mathrm{d}\,(\mathrm{d}\Phi.\Gamma_2).\Gamma_1(W) \\ \qquad - \frac{1}{6}B\,\Sigma\,\mathrm{d}\,(\mathrm{d}\Psi_1(W).\Gamma_1).\Gamma_1(W). \end{cases}$$

With the one-dimensional relations (11), we have in particular

$$B\,\Phi = \overline{B}\,\partial_x\Phi = \overline{B}\,\partial_x(E(x)\,W) = \overline{B}\,\delta\,W.$$

Then $\Gamma_1 = \overline{A}\,\partial_x W + \overline{B}\,\delta\,W = \alpha_1\,W$ with $\alpha_1 = \overline{A}\,\partial_x + \overline{B}\,\delta$ and the first relation of the family (14) is proven. We have as previously $D\,\Phi = \overline{D}\,\partial_x(E(x)\,W) = \overline{D}\,\delta\,W$ and

$$\Psi_1(W) = \mathrm{d}\Phi(W).\Gamma_1(W) - \big(C\,W + D\,\Phi(W)\big) = E\,\alpha_1\,W - (\overline{C}\,\partial_x W + \overline{D}\,\delta\,W)$$
$$= \big[E\,\alpha_1 - (\overline{C}\,\partial_x + \overline{D}\,\delta)\big]\,W \equiv \beta_1\,W.$$

Then the second relation in (14) relative to β_1 is established.

From the fact that the matrix Σ is constant, we have now

$$\Gamma_2(W) = B\,\Sigma\,\Psi_1(W) = \overline{B}\,\partial_x\,\Sigma\,\beta_1\,W = \overline{B}\,\Sigma\,\partial_x\,\beta_1\,W \equiv \alpha_2\,W$$

and the relation in (14) relative to α_2 is proven.

When we differentiate the vector field $\Psi_1(W)$, we have $\mathrm{d}\Psi_1(W).\xi = \beta_1\,\xi$ and $\mathrm{d}\Psi_1(W).\Gamma_1(W) = \beta_1\,\alpha_1\,W$. Then

$$\Psi_2(W) = \Sigma\,\mathrm{d}\Psi_1(W).\Gamma_1(W) + \mathrm{d}\Phi(W).\Gamma_2(W) - D\,\Sigma\,\Psi_1(W)$$
$$= \Sigma\,\beta_1\,\alpha_1\,W + E\,\alpha_2\,W - \overline{D}\,\delta_x\,\Sigma\,\beta_1\,W = \big(\Sigma\,\beta_1\,\alpha_1 + E\,\alpha_2 - \overline{D}\,\Sigma\,\partial_x\,\beta_1\big)\,W \equiv \beta_2\,W$$

and the relation relation to β_2 in (14) is proven. We have also

$$B_2 = (A\,B + B\,D) = \overline{A}\,\partial_x\,\overline{B}\,\partial_x + \overline{B}\,\partial_x\,\overline{D}\,\partial_x = \big(\overline{A}\,\overline{B} + \overline{B}\,\overline{D}\big)\,\partial_x^2 = \overline{B}_2\,\partial_x^2.$$

In consequence,

$$\Gamma_3(W) = B\,\Sigma\,\Psi_2(W) + \tfrac{1}{12}B_2\,\Psi_1(W) - \tfrac{1}{6}B\,\mathrm{d}\Psi_1(W).\Gamma_1(W)$$
$$= \overline{B}\,\Sigma\,\partial_x\,\beta_2\,W + \tfrac{1}{12}\overline{B}_2\,\partial_x^2\,\beta_1\,W - \tfrac{1}{6}\overline{B}\,\partial_x\,\beta_1\,\alpha_1\,W$$
$$= \big(\overline{B}\,\Sigma\,\partial_x\,\beta_2 + \tfrac{1}{12}\overline{B}_2\,\partial_x^2\,\beta_1 - \tfrac{1}{6}\overline{B}\,\partial_x\,\beta_1\,\alpha_1\big)\,W \equiv \alpha_3\,W$$

and the expression of the operator α_3 in (14) is established. From the relation (34), we have $\mathrm{d}\big(\mathrm{d}\Psi_1(W).\Gamma_1(W)\big).\xi = \mathrm{d}\big(\beta_1\,\alpha_1\,W\big).\xi$ and $\mathrm{d}\big(\mathrm{d}\Psi_1(W).\Gamma_1(W)\big).\Gamma_1(W) = \beta_1\,\alpha_1\,\alpha_1\,W = \beta_1\,\alpha_1^2\,W$. Then

$$\Psi_3(W) = \Sigma\,\mathrm{d}\Psi_1(W).\Gamma_2(W) + \mathrm{d}\Phi(W).\Gamma_3(W) - D\,\Sigma\,\Psi_2(W) + \Sigma\,\mathrm{d}\Psi_2(W).\Gamma_1(W)$$
$$\quad + \tfrac{1}{6}D\,\mathrm{d}\Psi_1(W).\Gamma_1(W) - \tfrac{1}{12}D_2\,\Psi_1(W) - \tfrac{1}{12}\mathrm{d}\big(\mathrm{d}\Psi_1(W).\Gamma_1(W)\big).\Gamma_1(W)$$
$$= \Sigma\,\beta_1\,\alpha_2\,W + E\,\alpha_3\,W - \overline{D}\,\partial_x\,\Sigma\,\beta_2\,W + \Sigma\,\beta_2\,\alpha_1\,W$$
$$\quad + \tfrac{1}{6}\overline{D}\,\partial_x\,\beta_1\,\alpha_1\,W - \tfrac{1}{12}\overline{D}_2\,\partial_x^2\,\beta_1\,W - \tfrac{1}{12}\beta_1\,\alpha_1^2\,W$$
$$= \big(\Sigma\,\beta_1\,\alpha_2 + E\,\alpha_3 - \overline{D}\,\partial_x\,\Sigma\,\beta_2 + \Sigma\,\beta_2\,\alpha_1 + \tfrac{1}{6}\overline{D}\,\partial_x\,\beta_1\,\alpha_1 - \tfrac{1}{12}\overline{D}_2\,\partial_x^2\,\beta_1 - \tfrac{1}{12}\beta_1\,\alpha_1^2\big)\,W$$

and the relation (14) concerning β_3 is established.

We observe now that

$$B\,\mathrm{d}\,(\mathrm{d}\Phi.\Gamma_2).\xi = \overline{B}\,\partial_x\,\mathrm{d}(E\,\alpha_2\,W).\xi = \overline{B}\,\delta\,\alpha_2\,\xi \text{ and } B\,\mathrm{d}\,(\mathrm{d}\Phi.\Gamma_2).\Gamma_1(W) = \overline{B}\,\delta\,\alpha_2\,\alpha_1\,W.$$

We have finally

$$\Gamma_4(W) = B\,\Sigma\,\Psi_3(W) + \tfrac{1}{4}B_2\,\Psi_2(W) + \tfrac{1}{6}B\,D_2\,\Sigma\,\Psi_1(W) - \tfrac{1}{6}A\,B\,\Psi_2(W)$$
$$\quad - \tfrac{1}{6}B\,\mathrm{d}\,(\mathrm{d}\Phi.\Gamma_1).\Gamma_2(W) - \tfrac{1}{6}B\,\mathrm{d}\,(\mathrm{d}\Phi.\Gamma_2).\Gamma_1(W) - \tfrac{1}{6}B\,\Sigma\,\mathrm{d}\,(\mathrm{d}\Psi_1(W).\Gamma_1).\Gamma_1(W)$$
$$= \overline{B}\,\Sigma\,\partial_x\,\beta_3\,W + \tfrac{1}{4}\overline{B}_2\,\partial_x^2\,\beta_2\,W + \tfrac{1}{6}\overline{B}\,\overline{D}_2\,\Sigma\,\partial_x^3\,\beta_1\,W - \tfrac{1}{6}\overline{A}\,\overline{B}\,\partial_x^2\,\beta_2\,W$$
$$\quad - \tfrac{1}{6}\overline{B}\,\delta\,\alpha_1\,\alpha_2\,W - \tfrac{1}{6}\overline{B}\,\delta\,\alpha_2\,\alpha_1\,W - \tfrac{1}{6}\overline{B}\,\Sigma\,\partial_x\,\beta_1\,\alpha_1^2\,W$$
$$= \Big[\overline{B}\,\Sigma\,\partial_x\,\beta_3 + \tfrac{1}{4}\overline{B}_2\,\partial_x^2\,\beta_2 + \tfrac{1}{6}\overline{B}\,\overline{D}_2\,\Sigma\,\partial_x^3\,\beta_1 - \tfrac{1}{6}\overline{A}\,\overline{B}\,\partial_x^2\,\beta_2 - \tfrac{1}{6}\overline{B}\,\delta\,\alpha_1\,\alpha_2$$
$$\quad - \tfrac{1}{6}\overline{B}\,\delta\,\alpha_2\,\alpha_1 - \tfrac{1}{6}\overline{B}\,\Sigma\,\partial_x\,\beta_1\,\alpha_1^2\Big]\,W \equiv \alpha_4\,W$$

and the last relation of (14) giving the operator α_4 is explicated. $\qquad\square$

Annex B. Proof of Proposition 4

We start from the relations (14) that we write again which we rewrite for clarity of reading:

$$\begin{cases}
\alpha_1 = \overline{A}\,\partial_x + \overline{B}\,\delta \\
\beta_1 = E\,\alpha_1 - (\overline{C}\,\partial_x + \overline{D}\,\delta) \\
\alpha_2 = \overline{B}\,\Sigma\,\partial_x\,\beta_1 \\
\beta_2 = \Sigma\,\beta_1\,\alpha_1 + E\,\alpha_2 - \overline{D}\,\Sigma\,\partial_x\,\beta_1 \\
\alpha_3 = \overline{B}\,\Sigma\,\partial_x\,\beta_2 + \frac{1}{12}\,\overline{B_2}\,\partial_x^2\,\beta_1 - \frac{1}{6}\,\overline{B}\,\partial_x\,\beta_1\,\alpha_1 \\
\beta_3 = \Sigma\,\beta_1\,\alpha_2 + E\,\alpha_3 - \overline{D}\,\Sigma\,\partial_x\,\beta_2 + \Sigma\,\beta_2\,\alpha_1 + \frac{1}{6}\,\overline{D}\,\partial_x\,\beta_1\,\alpha_1 - \frac{1}{12}\,\beta_1\,\alpha_1^2 - \frac{1}{12}\,\overline{D_2}\,\partial_x^2\,\beta_1 \\
\alpha_4 = \overline{B}\,\Sigma\,\partial_x\,\beta_3 + \frac{1}{4}\,\overline{B_2}\,\partial_x^2\,\beta_2 + \frac{1}{6}\,\overline{B}\,\overline{D_2}\,\Sigma\,\partial_x^3\,\beta_1 - \frac{1}{6}\,\overline{A}\,\overline{B}\,\partial_x^2\,\beta_2 \\
\qquad - \frac{1}{6}\,\overline{B}\,\delta\,\alpha_1\,\alpha_2 - \frac{1}{6}\,\overline{B}\,\delta\,\alpha_2\,\alpha_1 - \frac{1}{6}\,\overline{B}\,\Sigma\,\partial_x\,\beta_1\,\alpha_1^2\,.
\end{cases}$$

With the D1Q3 lattice Boltzmann scheme, we have

$$\delta = \begin{pmatrix} \lambda\,\partial_u \\ \lambda^2\,\alpha\,\partial_x \end{pmatrix},\ E(x) = \begin{pmatrix} \lambda\,U\,\cos(k\,x) \\ \lambda^2\,\alpha \end{pmatrix},\ \Sigma = \begin{pmatrix} \sigma & 0 \\ 0 & \sigma' \end{pmatrix}$$

and

$$\overline{A} = 0\,,\ \overline{B} = (1\,,\,0)\,,\ \overline{C} = \begin{pmatrix} \frac{2\lambda^2}{3} \\ 0 \end{pmatrix},\ \overline{D} = \begin{pmatrix} 0 & \frac{1}{3} \\ \lambda^2 & 0 \end{pmatrix}.$$

Then we obtain $\alpha_1 = \delta = \lambda\,\partial_u$,

$$\beta_1 = \begin{pmatrix} u \\ \lambda^2\,\alpha \end{pmatrix} \lambda\,\partial_u - \begin{pmatrix} \frac{2\lambda^2}{3} \\ 0 \end{pmatrix}\partial_x - \begin{pmatrix} 0 & \frac{1}{3} \\ \lambda^2 & 0 \end{pmatrix}\begin{pmatrix} \lambda\,\partial_u \\ \lambda^2\,\alpha\,\partial_x \end{pmatrix} = \begin{pmatrix} \lambda\,u\,\partial_u - \frac{2}{3}\,\lambda^2\,\partial_x - \frac{\lambda^2}{3}\,\alpha\,\partial_x \\ \lambda^3\,\alpha\,\partial_u - \lambda^3\,\partial_u \end{pmatrix}$$

$$= \begin{pmatrix} \lambda\,u\,\partial_u - \frac{1}{3}\,\lambda^2\,(\alpha+2)\,\partial_x \\ \lambda^3\,(\alpha-1)\,\partial_u \end{pmatrix}$$

and the relation (17) is proven. We have for second order accuracy $\overline{B}\,\Sigma = (\sigma,\,0)$. Then $\alpha_2 = \sigma\,\partial_x\left[\lambda\,u\,\partial_u - \frac{\lambda^2}{3}\,(\alpha+2)\,\partial_x\right] = \lambda^2\,\sigma\,(\partial_u^2 - \frac{\alpha+2}{3}\,\partial_x^2)$.

For the microscopic variables, we have

$$\beta_2 = \begin{pmatrix} \sigma & 0 \\ 0 & \sigma' \end{pmatrix}\lambda^2\begin{pmatrix} \lambda\,u\,\partial_u - \frac{2}{3}\,\lambda^2\,\partial_x - \frac{\lambda^2}{3}\,\alpha\,\partial_x \\ \lambda^3\,\alpha\,\partial_u - \lambda^3\,\partial_u \end{pmatrix}\lambda\,\partial_u + \begin{pmatrix} u \\ \lambda^2\,\alpha \end{pmatrix}\lambda^2\,\sigma\,(\partial_u^2 - \frac{\alpha+2}{3}\,\partial_x^2)$$

$$-\lambda\begin{pmatrix} 0 & \frac{\sigma'}{3} \\ \lambda^2\,\sigma & 0 \end{pmatrix}\begin{pmatrix} u\,\partial_u - \frac{1}{3}\,\lambda^2\,(\alpha+2)\,\partial_x \\ \lambda^2\,(\alpha-1)\,\partial_u \end{pmatrix}.$$

For the first component,

$$\beta_2^1 = \sigma\left(\lambda\,u\,\partial_u - \frac{\alpha+2}{3}\,\lambda^2\,\partial_x\right)\lambda\,\partial_u + \lambda^2\,u\,\sigma\,(\partial_u^2 - \frac{\alpha+2}{3}\,\partial_x^2) - \lambda^3\,\frac{\sigma'}{3}\,\partial_x\,(\alpha-1)\,\partial_u$$

$$= 2\,\lambda^2\,\sigma\,u\,\partial_u^2 - \frac{\alpha+2}{3}\,\lambda^3\,\partial_x\,\partial_u - \lambda^2\,\frac{\alpha+2}{3}\,u\,\partial_x^2 - \lambda^3\,(\alpha-1)\,\frac{\sigma'}{3}\,\partial_x\,\partial_u$$

$$= \lambda^3\left[2\,\sigma\,\frac{u}{\lambda}\,\partial_u^2 - \left(\frac{\alpha+2}{3}\,\sigma - \frac{\alpha-1}{3}\,\sigma'\right)\partial_x\,\partial_u - \frac{\alpha+2}{3}\,\sigma\,\frac{u}{\lambda}\,\partial_x^2\right]$$

and for the second component

$$\beta_2^2 = \lambda^2\,\sigma'\,(\lambda\,(\alpha-1)\,\partial_u)\,\lambda\,\partial_u + \lambda^4\,\alpha\,\sigma\,(\partial_u^2 - \frac{\alpha+2}{3}\,\partial_x^2) - \lambda^4\,\sigma\,(\frac{u}{\lambda}\,\partial_u - \frac{\alpha+2}{3}\,\partial_x)$$

$$= \lambda^4\left[(\alpha-1)\,\sigma'\,\partial_u^2 + \alpha\,\sigma\,(\partial_u^2 - \frac{\alpha+2}{3}\,\partial_x^2) - \sigma\,(\partial_u^2 - \frac{\alpha+2}{3}\,\partial_x^2)\right]$$

$$= \lambda^4\,(\alpha-1)\,((\sigma+\sigma')\,\partial_u^2 - \frac{\alpha+2}{3}\,\sigma\,\partial_x^2).$$

Then the relations (18) are established. At third order, we have from (14),

$$\alpha_3 = \overline{B}\,\Sigma\,\partial_x\,\beta_2 + \tfrac{1}{12}\,\overline{B_2}\,\partial_x^2\,\beta_1 - \tfrac{1}{6}\,\overline{B}\,\partial_x\,\beta_1\,\alpha_1$$

$$= \sigma\,\partial_x\beta_2^1 + \tfrac{1}{12}\left(0,\tfrac{1}{3}\right)\partial_x\beta_1 - \tfrac{1}{6}\,\overline{B}\,\partial_x\begin{pmatrix}\lambda\,u\,\partial_u - \tfrac{2}{3}\,\lambda^2\,\partial_x - \tfrac{\lambda^2}{3}\,\alpha\,\partial_x \\ \lambda^3\,\alpha\,\partial_u - \lambda^3\,\partial_u\end{pmatrix}\lambda\,\partial_u$$

$$= \lambda^3\,\sigma\,\partial_x\left[2\,\sigma\,\tfrac{u}{\lambda}\,\partial_u^2 - \left(\tfrac{\alpha+2}{3}\,\sigma - \tfrac{\alpha-1}{3}\,\sigma'\right)\partial_x\,\partial_u - \tfrac{\alpha+2}{3}\,\sigma\,\tfrac{u}{\lambda}\,\partial_x^2\right] + \tfrac{1}{12}\,\tfrac{\lambda^3}{3}\,(\alpha-1)\,\partial_x^2\,\partial_u$$

$$\quad - \tfrac{\lambda}{6}\,\partial_x\left[\lambda\,u\,\partial_u - \tfrac{\alpha+2}{3}\,\lambda^2\,\partial_x\right]\lambda\,\partial_u$$

$$= \lambda^3\left[\left(2\,\sigma^2 - \tfrac{1}{6}\right)\partial_u^3 + \left[-\sigma\left(\tfrac{\alpha+2}{3}\,\sigma + \tfrac{\alpha-1}{3}\,\sigma'\right) + \tfrac{\alpha-1}{36} + \tfrac{\alpha+2}{18}\right]\partial_x^2\,\partial_u - \tfrac{\alpha+2}{3}\,\sigma^2\,\partial_u\,\partial_x^2\right]$$

$$= \lambda^3\left[\left(2\,\sigma^2 - \tfrac{1}{6}\right)\partial_u^3 + \left(\tfrac{\alpha+2}{3}\left(\tfrac{1}{6} - \sigma^2\right) + \tfrac{\alpha-1}{3}\left(\tfrac{1}{12} - \sigma\,\sigma'\right)\right)\partial_x^2\,\partial_u - \tfrac{\alpha+2}{3}\,\sigma^2\,\partial_u\,\partial_x^2\right]$$

and the relation (19) is proven. We have now

$$\beta_3 = \Sigma\,\beta_1\,\alpha_2 + E\,\alpha_3 - \overline{D}\,\Sigma\,\partial_x\,\beta_2 + \Sigma\,\beta_2\,\alpha_1 + \tfrac{1}{6}\,\overline{D}\,\partial_x\,\beta_1\,\alpha_1 - \tfrac{1}{12}\,\beta_1\,\alpha_1^2 - \tfrac{1}{12}\,\overline{D_2}\,\partial_x^2\,\beta_1$$

and we can precise these seven terms:

$$\Sigma\,\beta_1\,\alpha_2 = \begin{pmatrix}\sigma & 0 \\ 0 & \sigma'\end{pmatrix}\lambda\begin{pmatrix}\lambda^3\left[2\,\sigma\,\tfrac{u}{\lambda}\,\partial_u^2 - \left(\tfrac{\alpha+2}{3}\,\sigma - \tfrac{\alpha-1}{3}\,\sigma'\right)\partial_x\,\partial_u - \tfrac{\alpha+2}{3}\,\sigma\,\tfrac{u}{\lambda}\,\partial_x^2\right] \\ \lambda^4\,(\alpha-1)\left((\sigma+\sigma')\,\partial_u^2 - \tfrac{\alpha+2}{3}\,\sigma\,\partial_x^2\right)\end{pmatrix}\lambda^2\,\sigma\left(\partial_u^2 - \tfrac{\alpha+2}{3}\,\partial_x^2\right)$$

$$E\,\alpha_3 = \begin{pmatrix}u \\ \lambda^2\,\alpha\end{pmatrix}\lambda^3\left[\left(2\,\sigma^2 - \tfrac{1}{6}\right)\partial_u^3 + \left(\tfrac{\alpha+2}{3}\left(\tfrac{1}{6} - \sigma^2\right) + \tfrac{\alpha-1}{3}\left(\tfrac{1}{12} - \sigma\,\sigma'\right)\right)\partial_x^2\,\partial_u - \tfrac{\alpha+2}{3}\,\sigma^2\,\partial_u\,\partial_x^2\right]$$

$$-\overline{D}\,\Sigma\,\partial_x\,\beta_2 = -\begin{pmatrix}0 & \tfrac{1}{3} \\ \lambda^2 & 0\end{pmatrix}\begin{pmatrix}\sigma & 0 \\ 0 & \sigma'\end{pmatrix}\partial_x\begin{pmatrix}\lambda^3\left[2\,\sigma\,\tfrac{u}{\lambda}\,\partial_u^2 - \left(\tfrac{\alpha+2}{3}\,\sigma - \tfrac{\alpha-1}{3}\,\sigma'\right)\partial_x\,\partial_u - \tfrac{\alpha+2}{3}\,\sigma\,\tfrac{u}{\lambda}\,\partial_x^2\right] \\ \lambda^4\,(\alpha-1)\left((\sigma+\sigma')\,\partial_u^2 - \tfrac{\alpha+2}{3}\,\sigma\,\partial_x^2\right)\end{pmatrix}$$

$$\Sigma\,\beta_2\,\alpha_1 = \begin{pmatrix}\sigma & 0 \\ 0 & \sigma'\end{pmatrix}\begin{pmatrix}\lambda^3\left[2\,\sigma\,\tfrac{u}{\lambda}\,\partial_u^2 - \left(\tfrac{\alpha+2}{3}\,\sigma - \tfrac{\alpha-1}{3}\,\sigma'\right)\partial_x\,\partial_u - \tfrac{\alpha+2}{3}\,\sigma\,\tfrac{u}{\lambda}\,\partial_x^2\right] \\ \lambda^4\,(\alpha-1)\left((\sigma+\sigma')\,\partial_u^2 - \tfrac{\alpha+2}{3}\,\sigma\,\partial_x^2\right)\end{pmatrix}\lambda\,\partial_u$$

$$\tfrac{1}{6}\,\overline{D}\,\partial_x\,\beta_1\,\alpha_1 = \tfrac{1}{6}\begin{pmatrix}0 & \tfrac{1}{3} \\ \lambda^2 & 0\end{pmatrix}\partial_x\begin{pmatrix}\lambda\,u\,\partial_u - \tfrac{1}{3}\,\lambda^2\,(\alpha+2)\,\partial_x \\ \lambda^3\,(\alpha-1)\,\partial_u\end{pmatrix}\lambda\,\partial_u$$

$$-\tfrac{1}{12}\,\beta_1\,\alpha_1^2 = -\tfrac{1}{12}\begin{pmatrix}\lambda\,u\,\partial_u - \tfrac{1}{3}\,\lambda^2\,(\alpha+2)\,\partial_x \\ \lambda^3\,(\alpha-1)\,\partial_u\end{pmatrix}\lambda^2\,\partial_u^2$$

$$-\tfrac{1}{12}\,\overline{D_2}\,\partial_x^2\,\beta_1 = -\tfrac{\lambda^2}{12}\begin{pmatrix}1 & 0 \\ 0 & \tfrac{1}{3}\end{pmatrix}\partial_x^2\begin{pmatrix}\lambda\,u\,\partial_u - \tfrac{1}{3}\,\lambda^2\,(\alpha+2)\,\partial_x \\ \lambda^3\,(\alpha-1)\,\partial_u\end{pmatrix}.$$

Then the first component of β_3 is given by the relation

$$\beta_3^1 = \lambda^4\left[\tfrac{\alpha+2}{9}\left[-(1-\alpha)\,\sigma\,\sigma' + \left((\alpha+2)\,\sigma^2 + \tfrac{1}{4}\right)\right]\partial_x^3\right.$$

$$\quad + U\left[-2\,\tfrac{\alpha+2}{3}\,\sigma^2 + \tfrac{1-\alpha}{3}\,\sigma\,\sigma' + \tfrac{1+\alpha}{12}\right]\partial_x^2\,\partial_u - 2\,U\,\tfrac{\alpha+2}{3}\,\sigma^2\,\partial_u\,\partial_x^2$$

$$\quad \left. + \left[-2\,\tfrac{\alpha+2}{3}\,\sigma^2 + \tfrac{1-\alpha}{3}\left(2\,\sigma\,\sigma' + \sigma'^2 - \tfrac{1}{4}\right)\right]\partial_x\,\partial_u^2 + \left(5\,\sigma^2 - \tfrac{1}{4}\right)U\,\partial_u^3\right]$$

and the second is given by

$$\beta_3^2 = \lambda^5\left[\tfrac{1-\alpha}{3}\left[(\alpha+2)\,\sigma^2 + (1+2\,\alpha)\,\sigma\,\sigma' - \tfrac{1+\alpha}{4}\right]\partial_x^2\,\partial_u + (1-\alpha)\,\tfrac{\alpha+2}{3}\,\sigma\,(\sigma+\sigma')\,\partial_u\,\partial_x^2\right.$$

$$\quad \left. - (1-\alpha)\left(2\,\sigma^2 + 2\,\sigma\,\sigma' + \sigma'^2 - \tfrac{1}{4}\right)\partial_u^3\right].$$

The relation (20) is proven. Finally,

$$\alpha_4 = \overline{B}\,\Sigma\,\partial_x\,\beta_3 + \tfrac{1}{4}\,\overline{B_2}\,\partial_x^2\,\beta_2 + \tfrac{1}{6}\,\overline{B}\,\overline{D_2}\,\Sigma\,\partial_x^3\,\beta_1 - \tfrac{1}{6}\,\overline{A}\,\overline{B}\,\partial_x^2\,\beta_2 - \tfrac{1}{6}\,\overline{B}\,\delta\,\alpha_1\,\alpha_2$$

$$\quad - \tfrac{1}{6}\,\overline{B}\,\delta\,\alpha_2\,\alpha_1 - \tfrac{1}{6}\,\overline{B}\,\Sigma\,\partial_x\,\beta_1\,\alpha_1^2.$$

After some lines of algebra,

$$\frac{1}{\lambda^4}\,\alpha_4 = \left[\left(\tfrac{\alpha+2}{3}\right)^2 \sigma^3 + (\alpha-1)\,\tfrac{\alpha+2}{9}\,\sigma^2\,\sigma' - \tfrac{\alpha+2}{36}\,\alpha\,\sigma\right]\partial_x^4$$
$$+ \left[-2\,\tfrac{\alpha+2}{3}\,\sigma^3 + 2\,\tfrac{1-\alpha}{3}\,\sigma^2\,\sigma' + \tfrac{1-\alpha}{3}\,\sigma\,\sigma'^2 + \tfrac{1+2\alpha}{9}\,\sigma + \tfrac{\alpha-1}{12}\,\sigma'\right]\partial_x^2\,\partial_u^2$$
$$+ \left[-2\,\tfrac{\alpha+2}{3}\,\sigma^3 + \tfrac{1-\alpha}{3}\,\sigma^2\,\sigma' + \tfrac{7+5\alpha}{36}\,\sigma\right]\partial_u\,\partial_x^2\,\partial_u + \tfrac{\alpha+2}{3}\,\sigma\left(-2\,\sigma + \tfrac{1}{6}\right)\partial_u^2\,\partial_x^2 + \sigma\left(5\,\sigma^2 - \tfrac{3}{4}\right)\partial_u^4$$
$$= \left[\tfrac{\alpha+2}{9}\left((\alpha+2)\,\sigma^3 - (1-\alpha)\,\sigma^2\,\sigma' - \tfrac{\alpha}{4}\,\sigma\right)\partial_x^4\right.$$
$$+ \left[-2\,\tfrac{\alpha+2}{3}\,\sigma^3 + \tfrac{1-\alpha}{3}\left(2\,\sigma^2\,\sigma' + \sigma\,\sigma'^2 - \tfrac{1}{4}\,\sigma'\right) + \tfrac{1+2\alpha}{9}\,\sigma\right]\partial_x^2\,\partial_u^2$$
$$+ \left[-2\,\tfrac{\alpha+2}{3}\,\sigma^3 + \tfrac{1-\alpha}{3}\,\sigma^2\,\sigma' + \tfrac{7+5\alpha}{36}\,\sigma\right]\partial_u\,\partial_x^2\,\partial_u + \tfrac{\alpha+2}{3}\,\sigma\left(-2\,\sigma + \tfrac{1}{6}\right)\partial_u^2\,\partial_x^2 + \sigma\left(5\,\sigma^2 - \tfrac{3}{4}\right)\partial_u^4$$

and the relation (21) is established. This completes the proof. $\qquad\square$

References

[1] A. Augier, F. Dubois, L. Gouarin, B. Graille, "Linear lattice Boltzmann schemes for Acoustic: parameter choices and isotropy properties", *Computers and Mathematics with Applications*, volume 65, pages 845-863, 2013.

[2] A. Augier, F. Dubois, B. Graille, P. Lallemand, "On rotational invariance of lattice Boltzmann schemes", *Computers and Mathematics with Applications*, volume 67, pages 239-255, 2014.

[3] T. Bellotti, B. Graille, M. Massot, "Finite difference formulation of any lattice Boltzmann scheme", *Numerische Mathematik*, volume **152**, pages 1-40, 2022.

[4] J. E. Broadwell, "Shock structure in a simple discrete velocity gas", *Physics of Fluids*, volume 7, pages 1243-1247, 1964.

[5] S. Chapman, T.G. Cowling, *The mathematical theory of non-uniform gases*, Cambridge University Press, 1939.

[6] S. Chen, G. D. Doolen, "Lattice Boltzmann Method for Fluid Flows", *Annual Review of Fluid Mechanics*, vol. **30**, p. 329-364, 1998.

[7] F. Dubois, "Equivalent partial differential equations of a lattice Boltzmann scheme", *Computers and Mathematics with Applications*, vol. **55**, p. 1441-1449, 2008.

[8] F. Dubois, "Third order equivalent equation of lattice Boltzmann scheme", *Discrete and Continuous Dynamical Systems, A*, vol. **23**, p. 221-248, 2009.

[9] F. Dubois, "Nonlinear fourth-order Taylor expansion of lattice Boltzmann schemes", *Asymptotic Analysis*, volume 127, pages 297-337, 2022.

[10] F. Dubois, B.M. Boghosian, P. Lallemand, "General fourth-order Chapman–Enskog expansion of lattice Boltzmann schemes", *Computers and Fluids*, volume 266, article 106036, 11 pages, 2023.

[11] F. Dubois, P. Lallemand, "Towards higher order lattice Boltzmann schemes", *Journal of Statistical Mechanics, Theory and Experiment*, P06006, 2009.

[12] F. Dubois, P. Lallemand, "Quartic Parameters for Acoustic Applications of Lattice Boltzmann Scheme", *Computers and Mathematics with Applications*, volume 61, p. 3404-3416, 2011.

[13] F. Dubois, P. Lallemand, "On Single Distribution Lattice Boltzmann Schemes for the Approximation of Navier Stokes Equations", *Communications in Computational Physics*, volume 34, pages 613-671, 2023.

[14] J. H. Ferziger, M. Perić, R. L. Street *Computational methods for fluid dynamics*, 1996, fourth edition Springer 2019.

[15] R. Gatignol, "The hydrodynamical description for a discrete velocity model of gas", *Complex systems*, volume 1, pages 709-725, 1987.

[16] Z. Guo, C. Shu, *Lattice Boltzmann method and its applications in engineering*, World Scientific, 2013.

[17] M. Hénon, "Viscosity of a lattice gas", *Complex systems*, volume 1, pages 763-789, 1987.

[18] D. d'Humières, "Generalized lattice-Boltzmann equations", in *Rarefied Gas Dynamics: Theory and Simulations*, volume 159 of *AIAA Progress in Astronautics and Aeronautics*, pages 450-458, 1992.

[19] D. d'Humières, I. Ginzburg, M. Krafczyk, P. Lallemand, L.-S. Luo, "Multiple-relaxation-time lattice Boltzmann models in three dimensions", *Philosophical Transactions of the Royal Society A: Mathematical, Physical and Engineering Sciences*, volume 15, pages 437-451, 2002.

[20] D. d'Humières, I. Ginzburg, "Viscosity independent numerical errors for Lattice Boltzmann models: From recurrence equations to "magic" collision numbers", *Computers And Mathematics with Applications*, volume 58, pages 823-840, 2009.

[21] T. Krüger, H. Kusumaatmaja, A. Kuzmin, O. Shardt, G. Silva, E. M. Viggen, *The Lattice Boltzmann Method: Principles and Practice*, Springer Verlag, 2017

[22] P. Lallemand, L.-S. Luo, "Theory of the lattice Boltzmann method: dispersion, dissipation, isotropy, galilean invariance, and stability", *Physical Review E*, volume 61, p. 6546-6562, 2000.

[23] B. Lucquin, O. Pironneau, *Introduction to scientific computing*, Wiley, 1998.

[24] R. Mei, L.-S. Luo, P. Lallemand, D. d'Humières, "Consistent initial conditions for lattice Boltzmann simulations", *Computers and Fluids*, volume 35, pages 855-862, 2006.

[25] J. T. Oden, J. N. Reddy, *An introduction to the mathematical theory of finite elements*, 1976, Dover Publications, 2011.

[26] H. Otomo, B. M. Boghosian, F. Dubois, "Two complementary lattice-Boltzmann-based analyses for nonlinear systems", *Physica A*, volume 486, pages 1000-1011, 2017.

[27] Y. H. Qian, Y. Zhou, "On higher order dynamics in lattice-based models using Chapman-Enskog method", *Physical Review E*, vol. **61**, p. 2103-2106, 2000.

[28] D. H. Rothman, S. Zaleski, *Lattice-gas cellular automata; simple models of complex hydrodynamics*, Cambridge University Press, Aléa-Saclay collection, 1997.

[29] SageMath, the Sage Mathematics Software System (Version 7.5.1), The Sage Developers, http://www.sagemath.org, 2017.

[30] S. Succi, *The lattice Boltzmann equation for fluid dynamics and beyond*, Clarendon Press, 2001